Highly symmetric random one-dimensional spin models

V. L. Quito,[1,2,*] P. L. S. Lopes,[3,4] José A. Hoyos,[5] and E. Miranda [6]

[1]*Department of Physics and Astronomy, Iowa State University, Ames, Iowa 50011, USA*

[2]*National High Magnetic Field Laboratory, Florida State University, Tallahassee, Florida 32306, USA*

[3]*Stewart Blusson Quantum Matter Institute, University of British Columbia, Vancouver, British Columbia, Canada V6T 1Z4*

[4]*Département de Physique, Institut Quantique and Regroupement Québécois sur les Matériaux de Pointe,*
Université de Sherbrooke, Sherbrooke, Québec, Canada J1K 2R1

[5]*Instituto de Física de São Carlos, Universidade de São Paulo, CP 369, São Carlos, São Paulo 13560-970, Brazil*

[6]*Gleb Wataghin Physics Institute, University of Campinas, Rua Sérgio Buarque de Holanda 777, CEP 13083-859 Campinas, São Paulo, Brazil*

The interplay of disorder and interactions is a challenging topic of condensed matter physics, where correlations are crucial and exotic phases develop. In one spatial dimension, a particularly successful method to analyze such problems is the strong-disorder renormalization group (SDRG). This method, which is asymptotically exact in the limit of large disorder, has been successfully employed in the study of several phases of random magnetic chains. Here we develop an SDRG scheme capable of providing in-depth information on a large class of strongly disordered one-dimensional magnetic chains with a global invariance under a generic continuous group. Our methodology can be applied to any Lie-algebra valued spin Hamiltonian, in any representation. As examples, we focus on the physically relevant cases of SO(N) and Sp(N) magnetism, showing the existence of different randomness-dominated phases. These phases display emergent SU(N) symmetry at low energies and fall into two distinct classes, with meson-like or baryon-like characteristics. Our methodology is here explained in detail and helps to shed light on a general mechanism for symmetry emergence in disordered systems.

I. INTRODUCTION

Magnetism carries a historical reputation as a useful platform to study quantum phases and transitions [1]. The convenience of magnetism does not arise from simple chance or tradition; it comes from the easiness with which one defines symmetries and their breaking, their accuracy in describing experimental results, and the inherent importance of quantum fluctuations. In particular, in one spatial dimension powerful tools, which are unavailable or less potent in higher dimensions, can be employed to gain useful insight on these important systems. Spin chains are set apart as a truly ideal playground in this regard.

An ingredient whose importance should not be underestimated in phase transitions is disorder [2]. Disorder is not only intrinsic to real physical materials, playing fundamental roles in the determination of transport properties; it may also stabilize distinctive phases with no analog in clean systems. The random singlet phase (RSP) in the disordered spin-1/2 XXZ model is the prototypical example [3]. RSPs are characterized by ground states composed of randomly distributed and arbitrarily long singlets. They are infinite-disorder phases, where there is a striking distinction between the average and typical values of spin correlation functions: while the latter decay as stretched exponentials $\sim e^{-r^\psi}$ with the distance r between spins, the former fall off as power laws $\sim r^{-\eta}$. The universal tunneling exponent ψ controls not only correlation functions but also thermodynamic quantities, like the

magnetic susceptibility and specific heat. In the paradigmatic XXZ spin-1/2 chain, the tunneling exponent attains a value of $\psi = 1/2$, while $\eta = 2$ [3].

From the statistical mechanics viewpoint (of classifying universality classes), an infinite-randomness fixed point is an interesting concept in its own right. In fact, infinite-randomness fixed points are much more common than originally thought. As critical points, they govern a plethora of phase transitions ranging from classical transitions in layered magnets [4], passing through quantum phase transitions in Ising magnets [5], higher-spin chains [6,7], and quantum rotors [8], to nonequilibrium phase transitions in epidemic-spreading models [9] (for more examples, see, e.g., the reviews in Refs. [2]). In addition, they can occur in all spatial dimensions [10–12]. In contrast, there are few examples of infinite-randomness fixed points describing stable phases of matter. To the best of our knowledge, the only examples are the RSPs of the spin-1/2 XXZ and higher-spin Heisenberg chains [3,13–17], the permutation-symmetric phases in non-Abelian anyonic chains [18,19], and the so-called mesonic and bosonic RSPs in the SU(2)-symmetric spin-1 chains [20].

The stable RSPs of the spin-1/2 XXZ and spin-1 chains are particularly noteworthy as they comprise examples of phases displaying symmetry emergence, where the low-energy and long-wavelength physics of a system are described by a larger symmetry than its microscopic description. As the main result of this work, we uncover a unifying framework in which the symmetry-enlarged infinite-randomness RSPs of the spin-1/2 XXZ chain and of the spin-1 chain are the simplest examples. The key observation for this unification is not to look at arbitrary-spin representations of SU(2), but rather at

---

*victorluizquito@gmail.com

the fundamental vector representations of SO(N). We show that SO(N)-symmetric random spin chains, in the strong-disorder limit, realize two distinct RSPs: a meson-like one, in which the tunneling exponent is $\psi_M = \frac{1}{2}$, and a baryon-like one, with $\psi_B = \frac{1}{N}$ (for $N > 1$). In both cases, correlations are invariant under the larger SU(N) group, with the mean correlations decaying algebraically with universal exponent $\eta = 2$. For odd N, there is a direct transition between these two RSPs which is governed by an unstable SU(N)-symmetric infinite-randomness fixed point with baryon-like tunneling exponent ψ_B.

To obtain these results, we rely on the strong-disorder renormalization group (SDRG) [21–23] (for a review, see Refs. [2,24]). The SDRG method consists of a sequential decimation of local strongly bound spins in a chain with random exchange couplings. It is a real-space RG method which allows one to keep track of the distributions of couplings under coarse graining. The stronger the disorder (i.e., the larger the variance of the distribution of coupling constants), the higher the accuracy of the method. When the fixed point is of the infinite-randomness kind, the method is capable of capturing the corresponding long-wavelength singular behavior exactly. In one spatial dimension, even analytic solutions are possible. We extend here the SDRG methodology, incorporating a general set of tools to handle arbitrary Lie groups that turns out to be remarkably powerful. As we demonstrate, these can be used to conveniently apply the SDRG to disordered Hamiltonians valued at any desired Lie algebras; analytical expressions can be derived for decimation rules and a natural basis is found for the coupling constants so that their RG flow is maximally decoupled allowing for a simple fixed-point analysis. This way, we see that our unifying framework is even more general. For concreteness, we pay particular attention to the SO(N)- and Sp(N)-invariant Hamiltonians and find that the Sp(N)-invariant chains also have RSPs in their phase diagrams. Unlike the SO(N) chains, however, we find only meson-like random-singlet phases. Finally, and more interestingly, we show that the baryonic SO(N)-symmetric RSPs and the mesonic SO(N)- and Sp(N)-symmetric RSPs exhibit the previously mentioned emergent (enlarged) SU(N) symmetry. That is, the ground state and the low-energy excitations are composed of SU(N)-symmetric objects [25]. As a consequence, susceptibilities and correlation functions (or any other observable) show emergent SU(N) symmetry. We focus on SO(N) and Sp(N) groups but we emphasize that Hamiltonians invariant under any Lie group can be approached by our methods.

We would like to emphasize that SO(N) magnetism is not as exotic as one might believe at first. Isomorphisms between algebras can be used to relate seemingly hard to realize orthogonal symmetries to very familiar ones. The first example is the well-known isomorphism between so(3) and su(2), which applies to the spin-1 chains where the symmetry emergence SU(2) → SU(3) was first studied [20]. The XXZ spin-1/2 chain can be viewed as a realization of the isomorphism between u(1) and so(2), with symmetry emergence U(1) → SU(2). Another example is the algebra isomorphism so(4) = su(2) ⊗ su(2), the latter being realized in the Kugel-Khomskii model [26] and explored in more detail here. These and other cases reported in Ref. [27] place our present analysis as centrally relevant to many realizable systems.

This paper is organized as follows. In Sec. II, we discuss the broad picture of applicability of our findings. In Sec. III we summarize the necessary information from group theory, considering our particular cases of interest, the orthogonal and symplectic groups. This is a highly technical discussion and readers who wish to understand the SDRG flow and its analysis may choose to initially skip this section and return to it as seen fit. In Sec. IV, we display the SDRG decimation rules in closed form that can, in principle, be generalized to spin chains invariant under any Lie group rotations. In this same section we apply the results to SO(N) and Sp(N) symmetric Hamiltonians. In Sec. V, we construct the phase diagram of SO(N) and Sp(N) chains, using the examples of SO(4), SO(5), Sp(4), and Sp(6). The SO(3) case [20] also fits in the same discussion, but is not revisited here. After that, we discuss the underlying mechanism of symmetry enhancement in Sec. VI, while some experimental predictions are given in Sec. VII. To contrast with the whole discussion of the work, in Sec. VIII we discuss a counterexample where RSPs develop without symmetry emergence. Finally, we summarize our finds and comment on generalizations in Sec. IX.

II. APPLICABILITY TO PHYSICAL SCENARIOS

Even though SO(N) and Sp(N) models look rather abstract, several specific examples can be connected to readily known or realizable systems. Focusing on SO(N)-invariant chains, physical scenarios can be obtained relying on handy group isomorphisms, as we list next.

We start by listing the two cases already studied before. The first one is the XXZ spin-1/2 chain which is well known for its U(1) symmetry. Its Hamiltonian is

$$H = \sum_i J_i \big(S_i^x S_{i+1}^x + S_i^y S_{i+1}^y + \Delta_i S_i^z S_{i+1}^z \big), \qquad (1)$$

where $\mathbf{S}_i$ are spin-1/2 operators and J_i and Δ_i are coupling-constant and anisotropy parameters, respectively. Due to the isomorphism between the U(1) and SO(2) groups, the Hamiltonian (1) configures our first example of SO(N) magnetism (with $N = 2$).

For uncorrelated random couplings $J_i > 0$ and $-\frac{1}{2} < \Delta_i < 1$, Fisher showed that $\Delta_i \to 0$ under renormalization and the corresponding (critical) phase is an RSP [3]. Thus, the corresponding fixed point is that of the random XX chain. Even though the effective Hamiltonian does not exhibit SU(2) symmetry (realized only when $\Delta_i = 1$), the ground state and the corresponding low-energy singular behavior are SU(2) symmetric. Therefore, although not explicitly noticed previously, this is the first example of the SO(N) → SU(N) symmetry-enhancement phenomenon in random systems.

The second case comes from the SU(2)-symmetric spin-1 chain, the Hamiltonian of which is

$$H = \sum J_i [\cos \theta_i \mathbf{S}_i \cdot \mathbf{S}_{i+1} + \sin \theta_i (\mathbf{S}_i \cdot \mathbf{S}_{i+1})^2], \qquad (2)$$

where $\mathbf{S}_i$ are spin-1 operators and J_i and θ_i are parameters. Here, the isomorphism between the SO(3) and SU(2) groups also plays a role. The SO(3) tensors can be understood, in the SU(2) language, as quadrupolar operators constructed out of spin-1 vectors. Hence, the Hamiltonian (1) is our second example of SO(N) magnetism (now with $N = 3$).

For uncorrelated random couplings J_i and parameters θ_i, it was shown that two RSPs exist in this model and that their corresponding fixed points do not exhibit SU(3) symmetry. However, like in the XXZ spin-1/2 chain, the corresponding ground states and low-energy singular behavior are SU(3) symmetric [20]. Although this was previously reported as an SU(2) $\rightarrow$ SU(3) symmetry enhancement, in this work this is just another example of the SO(N) $\rightarrow$ SU(N) phenomenon in random systems.

Having reviewed all the cases of SO(N) $\rightarrow$ SU(N) symmetry-enhancement in disordered spin chains previously studied in the literature, we now unveil another example of this phenomenon. By analogy, the next simplest scenario is that for $N = 4$, which is identified with the disordered version of the Kugel-Khomskii Hamiltonian [26]. In this model, each site has two orbital and two spin degrees of freedom. With the three components of spin operators **S** and the orbital degrees of freedom **T**, it is possible to construct the nine spin-orbital operators $S^a T^b$. The operators **S** and **T** can be chosen as the six generators of SO(4), while the collection of SO(4) and spin-orbital operators generate the SU(4) group. The choice of the spin and orbital vectors as generators of SO(4) comes from the isomorphism SO(4) $\sim$ SU(2) $\otimes$ SU(2). When the nine spin-orbital operators appear with the same coefficient as the three spin and orbital operators, the model becomes SU(4) invariant. In general,

$$H = \sum_i J_i (\boldsymbol{S}_i \cdot \boldsymbol{S}_j + a)(\boldsymbol{T}_i \cdot \boldsymbol{T}_j + a), \qquad (3)$$

where J_i are random numbers taken to be positive and $a = 1$ for SU(4) symmetry. If the coefficients of the spin-orbital operators are different from the spin and orbital ones, that is, $a \neq 1$, the global SU(4) symmetry is broken down to SO(4). In the general case, however, the Hamiltonian (3) configures our third example of SO(N) magnetism, here with $N = 4$.

By constructing a phase diagram as function of a, this model is found to flow under the SDRG to a nontrivial RSP exhibiting enhanced SU(4) symmetry governed by an infinite-randomness fixed point with $a = 0$.

Another physically relevant case is the SO(6)-invariant chains. As a consequence of the isomorphism between SO(6) and SU(4) groups, this can be physically realized with ultracold alkaline-earth atoms in the SU(4) context [28]. In the presence of disorder, an RSP can be stabilized exhibiting enlarged SU(6) symmetry. In other words, the SU(4)-symmetric spin chain in its six-dimensional representation (two horizontal boxes, in Young-tableau notation) is also SO(6) symmetric and displays SU(6)-symmetric RSP physics.

Finally, SO(N) chains can also be constructed from SU(2)-symmetric spin-S chains, with $N = 2S + 1$. The construction is not generic, however, as it requires fine tuning since larger degeneracies of the multiplets of two coupled spins are required [17].

III. LIE GROUPS TOOL KIT

The analyses of renormalization group (RG) flows always benefit from a clever parametrization of coupling constants, ideally one that decouples the flow of the variables as much as

TABLE I. A summary of our notation conventions.

Notation	Description
Υ	Irreducible representations
υ	Intra-representation-state labels
$\mathbf{L}_i / \mathbf{M}_i / \boldsymbol{\Lambda}_i$	SO(N)/Sp(N)/SU(N) spins on site i in a given representation
$T_\upsilon^\Upsilon(\mathbf{L}_i)$	Irreducible tensor operator of rank Υ, component υ, as a function of $\mathbf{L}_i$
$\mathcal{O}^\Upsilon(\mathbf{L}_i, \mathbf{L}_j)$	Scalar operator built out of tensors of rank Υ on the link (i, j) defined by corresponding spins
$K^{(1)}, K^{(2)}$	SO(N)/Sp(N) coupling constants

possible. The SDRG, with a thermodynamically infinite number of coupling constants, is no different. The optimal choice is determined by symmetry considerations: a proper language keeps the covariance of the Hamiltonian under the RG steps explicit, and is such that the decimation rules can be computed in an as-easy-as-possible way. Such an ideal language for the SDRG will be introduced here. It takes the form of a tool kit of Lie groups and algebras, particularizing for our purposes to the cases of SO(N) and Sp(N). Generally, using this tool kit one may derive the SDRG decimation steps of spin Hamiltonians in any representation of any group. We would like to emphasize, once again, that this and the next sections are rather technical and dedicated to the development of a collection of tools of broad interest in disordered chains. The reader who is interested in the specific cases of SO(N) and Sp(N) can skip this and the next sections, while using Table I to understand the notation used in this work, whenever necessary.

The tools in our set comprise the following: (i) Lie algebras and their unique representation label scheme. (ii) Irreducible tensor operators lying within a given representation [i.e., a generalization of the familiar SU(2) irreducible tensor operators, naturally built out of spherical harmonics] [17]. (iii) The corresponding group-invariant scalars for each representation. These scalars permit a convenient construction of the most general group-invariant Hamiltonian. (iv) The Wigner-Eckart theorem, which brings out the full value of the points above in the SDRG method. It ensures independent coupling constant RG flows for each different scalar operator that appears in the spin Hamiltonian. This theorem, applicable to any Lie group [29], allows one to easily compute the matrix elements of the irreducible tensor operators, and allows the perturbation theory steps of the SDRG decimation to be performed easily.

This section is quite mathematical, but necessary for what follows; the general exposition here follows the conventions of Ref. [29]. In order to keep the discussion less abstract, we introduce most concepts using the SO(N) group as a prototype, the Sp(N) case following more easily. The notation used throughout the paper is listed in Table I.

A. SO(N) group

1. Group structure and representation labeling

The SO(N) group is defined by the set of orthogonal $N \times N$ matrices satisfying

$$O O^T = O^T O = 1, \quad \det O = 1. \qquad (4)$$

TABLE II. Labeling of SO(N) representations. A set of integers must be attributed to each case following a hierarchy as displayed. SO(2) and SO(3) cases are well known, from the z component and the magnitude squared of the angular-momentum vector operator, respectively. For higher N, the number of integers necessary to uniquely label representations increases by one for every two values of N.

SO(2)	$[\mu_1] \leftrightarrow M$
SO(3)	$[\mu_1] \leftrightarrow J$
SO(4)	$[\mu_1, \mu_2], \mu_1 \geqslant |\mu_2| \geqslant 0$
SO(5)	$[\mu_1, \mu_2], \mu_1 \geqslant \mu_2 \geqslant 0$

The O matrices admit an exponential description as $O = e^{iA}$, where, from Eq. (4), $A^T = -A$ and $\text{Tr}A = 0$. Choosing a unitary representation, the antisymmetric A matrices are Hermitian, and thus purely imaginary. A complete basis for these matrices has $d_{SO} = N(N-1)/2$ elements L^{ab}, the group generators [30]. Therefore, one can write the A matrices as linear combinations with real coefficients ξ_{ab} as

$$A = \sum_{a,b} \xi_{ab} L^{ab}, \tag{5}$$

where a normalization choice is made according to which $\text{Tr}(L^{ab}L^{cd}) = 2(\delta^{ac}\delta^{bd} - \delta^{ad}\delta^{bc})$. Combining Eqs. (5) and (4), and expanding to first order in ξ_{ab}, one obtains the so(N) Lie algebra

$$[L^{ab}, L^{cd}] = i(\delta^{ac}L^{bd} + \delta^{bd}L^{ac} - \delta^{ad}L^{bc} - \delta^{bc}L^{ad}). \tag{6}$$

The distinct sets of matrices that satisfy (6) are the representations of the algebra/group, which requires a unique labeling scheme. SO(N) representations separate into tensor and spinor representations. Since here we are interested only in the former, from now on, when we talk about SO(N) representations we will be referring to tensor representations. SO(N) representations can be denoted by a set of integers: $\Upsilon \equiv [\mu_1, \mu_2, \ldots, \mu_\nu]$, with $\nu = \text{int}(N/2)$. These integers are such that for odd N, $\mu_1 \geqslant \mu_2 \geqslant \cdots \geqslant \mu_\nu \geqslant 0$, whereas for even N, $\mu_1 \geqslant \mu_2 \geqslant \cdots \geqslant |\mu_\nu| \geqslant 0$ [29]. Equivalently, these $\{\mu_i\}$ can be used to ascribe a Young tableau to each representation, with each integer representing the number of boxes in each row. As usual, antisymmetric representations correspond to a single column of boxes and, from the value of ν, we see that in SO(N), antisymmetric representations exist with at most $\text{int}(N/2)$ boxes. This is in contrast to the familiar SU(N) case, where a column of up to $N-1$ boxes is allowed.

To help familiarize the reader, some examples are shown in Table II. The cases of SO(2) and SO(3) can be understood from the standard angular-momentum physics. SO(2) representations are labeled by a single set of integers, both positive and negative valued, $[\mu_1] \leftrightarrow M$, $|M| \geqslant 0$, which are nothing but the eigenvalues of the z component of the angular-momentum operator. This is because the Abelian group of two-dimensional rotations in the xy plane admits only one-dimensional representations with basis vectors $\psi_M(\phi) = e^{iM\phi}$. As for SO(3), the representations are again given by a single number, but now only positive integers are allowed $[\mu_1] \leftrightarrow J$, which, from standard knowledge, have a unique correspondence to the square of the angular-momentum vec-

tor operator. The next natural example is SO(4), but due to some caveats unique to this group, we postpone its discussion for later. Moving on to SO(5), two integers become necessary to identify a representation. For example, $[0, 0]$ is the singlet with dimension $d_{[0,0]} = 1$; $[1, 0]$ is the fundamental vector (or defining) representation with dimension $d_{[1,0]} = 5$ and is represented by a single box in Young-tableau language. Examples of antisymmetric and symmetric representations are, respectively, $[1, 1]$ and $[2, 0]$, with dimensions $d_{[1,1]} = 10$ and $d_{[2,0]} = 14$. They are alternatively represented, respectively, by two vertically and two horizontally arranged boxes in Young-tableau language. This structure for defining antisymmetric and symmetric representations is general for all N. As we move on in the text, we refer to the representations interchangeably in the notation of Υ, the dimension of the representation or the corresponding Young tableau, as dictated by convenience.

2. SO(N) Hamiltonians and tensor operators

With the definition of the SO(N) group and a choice of representation, we now show how to write down the most

$$H_{ij} = J_{ij}(\boldsymbol{L}_i \cdot \boldsymbol{L}_j) + D_{ij}(\boldsymbol{L}_i \cdot \boldsymbol{L}_j)^2, \tag{7}$$

where $\boldsymbol{L}_i \cdot \boldsymbol{L}_j \equiv \sum_{a<b} L_i^{ab} L_j^{ab}$. Powers of the dot product greater than 2 are linearly dependent on lower powers [31]. For the third power, for instance,

$$(\boldsymbol{L}_i \cdot \boldsymbol{L}_j)^3 = \boldsymbol{L}_i \cdot \boldsymbol{L}_j + (1-N)(\boldsymbol{L}_i \cdot \boldsymbol{L}_j)^2 + N - 1. \tag{8}$$

The SDRG method relies extensively on perturbation theory calculations involving the projection of the spin operators on certain representations. While Eq. (7) is easy to build, projection calculations are much more conveniently performed if one works in the language of *irreducible tensor operators*. This was first noticed in Ref. [32] and extensively applied in Ref. [17]. For SO(3) $\sim$ SU(2) this is the language of irreducible spherical tensors of standard quantum mechanics textbooks [33]. Here we discuss the general Lie group case.

General tensor operators T_υ^Υ are defined as satisfying [29]

$$\left[L^{ab}, T_\upsilon^\Upsilon\right] = \sum_{\upsilon'} \langle \Upsilon \upsilon' | L^{ab} | \Upsilon \upsilon \rangle T_{\upsilon'}^\Upsilon. \tag{9}$$

The labels Υ, that previously were used to uniquely define a representation, also specify a tensor rank. The set of labels υ, on the other hand, is used to uniquely specify both a state within a given representation and a component of a tensor operator. In the usual scenario of SO(3) $\sim$ SU(2), υ is then the eigenvalue of the z component of the angular-momentum operator which can be chosen to be, for example, L^{12}. For larger N, a larger collection of labels is again required to specify υ. For us, they can be generically chosen as a set of eigenvalues of the *Cartan subalgebra*, that is, the eigenvalues of the maximal subset of commuting generators, i.e., that can be simultaneously diagonalized. In general, for SO(N), the Cartan subalgebra contains $\text{int}(N/2)$ generators. These eigenvalues are known as *weights*.

The set of group generators can be broken down into the Cartan subalgebra generators and the remaining set. From this remaining set, generators can be linearly combined to produce the so-called *root operators*, that allow one to move among
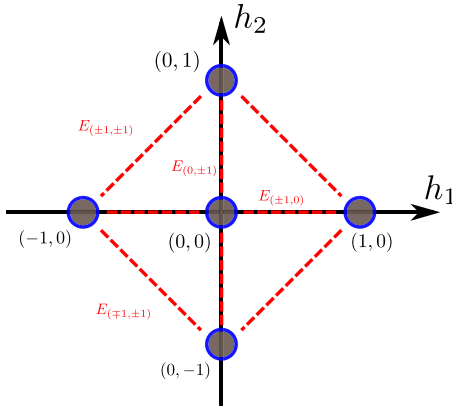
FIG. 1. Roots and weights for the fundamental representation of the SO(5) group. The weights are obtained by diagonalizing the set of operators that span the Cartan subalgebra and are used to uniquely define a state within a given representation (in this case, the fundamental one). In SO(5), there are int($N/2$) = 2 Cartan generators and their eigenvalues, the weight vectors $\boldsymbol{v} = (h_1, h_2)$ (blue circles), are two-dimensional. The E operators are the root operators and connect distinct weights (dashed red lines).

different weights. These are the usual angular-momentum raising and lowering operators in the SO(3) $\sim$ SU(2) case. As an example, for SO(5), the root/weight diagram of the fundamental representation is shown in Fig. 1. While for a given N the number of root operators is always the same, the weights depend on the representation.

Every representation Υ admits a conjugate representation with which it can be combined to build SO(N)-invariant objects, or *scalar operators*, by contraction [29]. These scalar operators allow us to simplify the analysis of the SDRG flow dramatically. For the SO(N) group, they are given by

$$\mathcal{O}^{\Upsilon}(\boldsymbol{L}_i, \boldsymbol{L}_j) = \sum_{\upsilon} (-1)^{f(\Upsilon, \upsilon)} T_{\upsilon}^{\Upsilon}(\boldsymbol{L}_i) T_{-\upsilon}^{\Upsilon}(\boldsymbol{L}_j), \quad (10)$$

where $-\upsilon$ and the phase $f(\Upsilon, \upsilon)$ are fixed by the requirement that $\mathcal{O}^{\Upsilon}$ be a scalar; i.e., it must satisfy $[\mathcal{O}^{\Upsilon}, \boldsymbol{L}_i + \boldsymbol{L}_j] = \boldsymbol{0}$, computed using (9). In SO(3), for instance, $\upsilon = M$, $\Upsilon = J$, and $f(J, M) = M$.

Starting with tensors, one can systematically write down group-invariant spin Hamiltonians using scalar operators as desired. To fix how many scalars appear in a given Hamiltonian, all one needs to do is consider the tensor product of the spins in the desired representations at sites i, j. The number of terms in the Hamiltonian matches the number of terms in this Clebsch-Gordan series. For example, when two defining representations of the SO(N) group are combined, the Clebsch-Gordan series has three terms [34],

$$[1, \vec{0}] \otimes [1, \vec{0}] = [\vec{0}] \oplus [1, 1, \vec{0}] \oplus [2, \vec{0}], \quad (11)$$

where the $\vec{0}$ vectors contain as many zeros as necessary to complete int($N/2$). The tensor corresponding to $\mathcal{O}^{[\vec{0}]}$ is just a constant and can be neglected. We conclude, therefore, that the most general SO(N) Hamiltonian contains two scalar operators $\mathcal{O}^{(1)} \equiv \mathcal{O}^{[1,1]}$ and $\mathcal{O}^{(2)} \equiv \mathcal{O}^{[2,0]}$, the same number of terms as discussed before in Eq. (7). Figure 2 displays the
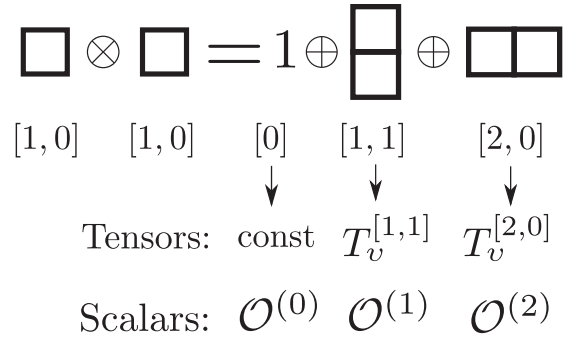

FIG. 2. Schematic representation of how to build SO(N) scalars, starting from the Young-tableau representation of the Clebsch-Gordan series. We use as an example the product of two fundamental representations, since this is the relevant case for our purposes. First, associated with each representation Υ coming out of the Clebsch-Gordan series of two representations, there is a set of tensors, T_{υ}^{Υ}. These tensors of a given rank can be contracted yielding a scalar $\mathcal{O}^{\Upsilon}$. The most generic Hamiltonian of a pair of sites is a linear combination of the scalars.

schematic association of the lowest representations, tensors and scalars, as well as the Young-tableau notation of SO(N).

Having determined all the scalar operators, the most general group-invariant Hamiltonian is written as an arbitrary linear combination of them. Restricting interactions to first neighbors only and neglecting constant terms, the Hamiltonian reads

$$H = \sum_i H_{i,i+1},$$

$$H_{i,i+1} = \sum_{\Upsilon} K_i^{\Upsilon} \mathcal{O}^{\Upsilon}(\boldsymbol{L}_i, \boldsymbol{L}_{i+1}). \quad (12)$$

To make the notation clearer, we define $\Upsilon = [0, 0] \equiv (0), [1, 1] \equiv (1), [2, 0] \equiv (2)$ as labels. Particularizing to SO(N) in its fundamental representation, only two terms contribute,

$$H_{i,i+1} = K_i^{(1)} \mathcal{O}^{(1)}(\boldsymbol{L}_i, \boldsymbol{L}_{i+1}) + K_i^{(2)} \mathcal{O}^{(2)}(\boldsymbol{L}_i, \boldsymbol{L}_{i+1}). \quad (13)$$

Using Eq. (9) to determine the exact structure of the tensor operators and their corresponding scalars in terms of spins $\boldsymbol{L}_i$ is computationally tedious and demanding. While $\mathcal{O}^{(1)}(\boldsymbol{L}_i, \boldsymbol{L}_{i+1}) = \boldsymbol{L}_i \cdot \boldsymbol{L}_{i+1}$ has a form reminiscent of the Heisenberg Hamiltonian for any group, $\mathcal{O}^{(2)}(\boldsymbol{L}_i, \boldsymbol{L}_{i+1})$ can have a more complicated (non-bilinear) structure. For SO(N) [and Sp(N) below], however, a fortunate shortcut exists. The trick is to take advantage of the SU(N) group, of which both SO(N) and Sp(N) are subgroups.

The SU(N) group has $N^2 - 1$ generators we will call Λ^{μ}. As discussed, the lowest-order nontrivial SU(N) scalar operator is $\mathcal{O}^{(1)}$ [35];

$$H_{i,j}^{SU(N)} = \sum_{\mu=1}^{N^2-1} \Lambda_i^{\mu} \Lambda_j^{\mu} = \boldsymbol{\Lambda}_i \cdot \boldsymbol{\Lambda}_j. \quad (14)$$

As the unitary algebra contains the orthogonal one, su(N) $\supset$ so(N), we can focus on the $N(N-1)/2$ purely imaginary generators of SU(N) which are, in fact, the d_{SO} generators

of the SO(N) group ($\Lambda_i^\mu = L_i^{ab}$). Labeling these with $\mu = 1, \ldots, d_{SO}$, this simple observation allows us to write

$$\mathcal{O}^{(1)}(\boldsymbol{L}_i, \boldsymbol{L}_j) = \boldsymbol{L}_i \cdot \boldsymbol{L}_j \equiv \sum_{\mu=1}^{d_{SO}} \Lambda_i^\mu \Lambda_j^\mu. \tag{15}$$

The SU(N)-invariant Hamiltonian (14) must also be SO(N) invariant and, since $\mathcal{O}^{(1)}$ was built out of the $N(N-1)/2$ purely imaginary generators, the remaining terms in it must immediately give us $\mathcal{O}^{(2)}$. Indeed, $\mathcal{O}^{(2)}$ can be decomposed as

$$\mathcal{O}^{(2)}(\boldsymbol{L}_i, \boldsymbol{L}_j) = \sum_{\mu=d_{SO}+1}^{N^2-1} \Lambda_i^\mu \Lambda_j^\mu$$
$$= \boldsymbol{L}_i \cdot \boldsymbol{L}_j + \frac{2}{N-2}(\boldsymbol{L}_i \cdot \boldsymbol{L}_j)^2, \tag{16}$$

where the coefficients can be found by direct computation [36]. Computationally, working with SU(N) matrices is a much easier task than the complete determination of $\mathcal{O}^{(2)}$ by means of the route given in Fig. 2 and Eqs. (9) and (10). This process provides us with the Hamiltonian in terms of $\mathcal{O}^{(1)}$ and $\mathcal{O}^{(2)}$ without ever writing the tensor operators explicitly.

Allowing for disorder to define site-dependent couplings, the disordered SO(N)-invariant Hamiltonian becomes

$$H = \sum_i \left[K_i^{(1)} \mathcal{O}^{(1)}(\boldsymbol{L}_i, \boldsymbol{L}_{i+1}) + K_i^{(2)} \mathcal{O}^{(2)}(\boldsymbol{L}_i, \boldsymbol{L}_{i+1}) \right], \tag{17}$$

with $\mathcal{O}^{(1)}$ and $\mathcal{O}^{(2)}$ given in Eqs. (15) and (16), and $K_i^{(1)} = J_i - \frac{N-2}{2}D_i$, $K_i^{(2)} = \frac{N-2}{2}D_i$ [if one wishes to compare with the notation Eq. (7)]. As a final remark, note that the most general SO(N)-symmetric spin chain can be recast as a special anisotropic SU(N) spin chain. This realization is very useful when analyzing the RG flow.

B. Sp(N)

Much of the previous analysis is in fact group and algebra independent, so we can be more concise for the Sp(N) case. We restrict ourselves to introducing the group, making a few comments, and moving straight to the most general Hamiltonian, which can be found in a procedure similar to that described above. A general element of Sp(N), where N is assumed to be even, satisfies the symplectic relation

$$U^T J U = J, \quad J = \begin{pmatrix} 0 & I \\ -I & 0 \end{pmatrix}, \tag{18}$$

where I is the $N/2$-dimensional identity matrix. Writing $U = \exp(i\theta \cdot \mathbf{M})$, and expanding to first order in $\mathbf{M}$, we find

$$(\theta \cdot \mathbf{M})^T J + J(\theta \cdot \mathbf{M}) = 0. \tag{19}$$

Following reasoning similar to what was implemented for SO(N), we are able to build tensor operators. First, the scalar $\mathcal{O}^{(1)}$ is constructed by contracting all the $d_{Sp} = N(N+1)/2$ Sp(N) generators. These generators can be identified with some SU(N) operators, which is guaranteed by Sp(N) $\subset$ SU(N). Analogously to the SO(N) case, $\mathcal{O}^{(2)}$ can be constructed with the remaining $N(N-1)/2 - 1$ SU(N)

generators. Thus,

$$\mathcal{H} = \sum_i \left(K_i^{(1)} \sum_{\mu=1}^{d_{Sp}} \Lambda_i^\mu \Lambda_{i+1}^\mu + K_i^{(2)} \sum_{\mu=d_{Sp}+1}^{N^2-1} \Lambda_i^\mu \Lambda_{i+1}^\mu \right)$$
$$= \sum_i \left[K_i^{(1)} \mathcal{O}^{(1)}(\boldsymbol{M}_i, \boldsymbol{M}_{i+1}) + K_i^{(2)} \mathcal{O}^{(2)}(\boldsymbol{M}_i, \boldsymbol{M}_{i+1}) \right]. \tag{20}$$

Writing the explicit form of the scalar operators, we have

$$\mathcal{O}^{(1)}(\boldsymbol{M}_i, \boldsymbol{M}_j) = \boldsymbol{M}_i \cdot \boldsymbol{M}_j, \tag{21}$$

$$\mathcal{O}^{(2)}(\boldsymbol{M}_i, \boldsymbol{M}_j) = \boldsymbol{M}_i \cdot \boldsymbol{M}_j$$
$$+ \frac{1}{\frac{N}{2}+1}(\boldsymbol{M}_i \cdot \boldsymbol{M}_j)^2 - \frac{2(N+1)}{N\left(\frac{N}{2}+1\right)}. \tag{22}$$

C. Generalized Wigner-Eckart theorem

We now provide the final ingredient that, using the information above, allows one to derive SDRG rules: the Wigner-Eckart theorem. One may be familiar with this theorem from applications of group theory to selection rules for angular momentum, the particular case of the SU(2) $\sim$ SO(3) group. Here, we remind the reader that the theorem is valid for any Lie group and reads [29]

$$\langle \Upsilon_1 \upsilon_1 | T_\upsilon^\Upsilon | \Upsilon_2 \upsilon_2 \rangle = \langle \Upsilon_1 \upsilon_1 | \Upsilon \upsilon \Upsilon_2 \upsilon_2 \rangle \langle \Upsilon_1 \| T^\Upsilon \| \Upsilon_2 \rangle. \tag{23}$$

Again the matrix elements $\langle \Upsilon_1 \lambda_1 | \Upsilon \lambda \Upsilon_2 \lambda_2 \rangle$ are Clebsch-Gordan coefficients connecting the basis of the "added representation" (analogous to total angular momentum) with the basis that is formed by the tensor product of two representations (say, from distinct sites). The reduced matrix elements $\langle \Upsilon_1 \| T^\Upsilon \| \Upsilon_2 \rangle$ are independent of υ_1, υ_2, being constant for given Υ, Υ_1, and Υ_2. This factorization, in terms of Clebsch-Gordan coefficients and reduced matrix elements, simplifies the SDRG analysis dramatically and justifies *a posteriori* the introduction of these objects [37].

IV. STRONG-DISORDER RG DECIMATION RULES

In this section we derive the SDRG decimation rules for any spin system invariant under global Lie group transformations. For concreteness, in Secs. IV C and IV D we particularize our calculations for the SO(N)- and Sp(N)-symmetric spin chains, the corresponding Hamiltonians of which are (17) and (20), respectively. We emphasize that the process here described is general in the sense that it is independent of the representation and the number of scalar operators at each link.

The SDRG procedure starts by probing the chain for the most strongly coupled pair of spins. This is determined by the pair with the largest gap between ground and first excited multiplets (which we call the "local gap"). The assumed large variance of the distribution of couplings implies that with high probability, its neighboring links are much weaker. We thus focus on the 4-site problem

$$\mathcal{H} = \mathcal{H}_{1,2} + \mathcal{H}_{2,3} + \mathcal{H}_{3,4}, \tag{24}$$

assuming that $(2, 3)$ is the strongly coupled pair and considering $\mathcal{H}_{1,2} + \mathcal{H}_{3,4}$ as a small perturbation to $\mathcal{H}_{2,3}$. As we saw in
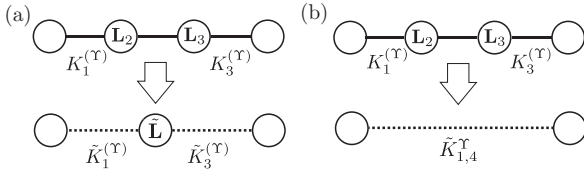
FIG. 3. Schematic representation of the SDRG decimation steps. Depending on whether the local ground multiplet of the spin pair on sites 2 and 3 is degenerate or not, decimations will follow respectively from first- [panel (a)] or second-order [panel (b)] perturbation theory. The ground multiplet is fixed by the values of K_2^{Υ}, the couplings corresponding to tensors of rank Υ. Couplings of different ranks are not mixed by the decimation.

Sec. III, we can write

$$\mathcal{H}_{2,3} = \sum_{\Upsilon} K_2^{\Upsilon} \mathcal{O}^{\Upsilon}(\mathbf{L}_2, \mathbf{L}_3). \tag{25}$$

In this section, with some abuse of notation, $\mathbf{L}_i$ stands for operators of any representation of any Lie group [or keep in mind SO(N) or Sp(N) for concreteness]. Also, as described ahead, at initial RG steps, $\mathbf{L}_i$ corresponds to the generators of the defining representation of the group, but as the RG proceeds, that need not be the case.

The crucial information to be obtained from (25) is its ground multiplet, which depends on the set of constants $\{K_2^{\Upsilon}\}$. The RG decimations project the Hamiltonian of each strongly bound pair of spins onto such ground multiplet, and two distinct classes of situations arise: either these representations are singlets (one-dimensional) or they transform as some other higher-dimensional representation. The SDRG will allow the group representations and coupling constants to flow according to which of these two cases happens for each pair of strongly bound spins, as we explain in the next subsections. A pictorial representation of these two possible decimation steps is shown in Fig. 3.

A. First-order perturbation theory

Let us assume that the energy of the strongly coupled sites 2 and 3 is great enough to justify freezing them in their two-spin ground multiplet. If the coupling constants $\{K_2^{\Upsilon}\}$ are such that this ground multiplet is degenerate, then the 4-site problem can be treated perturbatively as an effective 3-site problem. The middle site then corresponds to a spin object corresponding to the ground-state manifold of the previous (2, 3) link (see Fig. 3). Accordingly, its couplings to sites 1 and 4 (namely $\tilde{K}_1^{\Upsilon}$ and $\tilde{K}_3^{\Upsilon}$) receive corrections to first order in perturbation theory.

By symmetry, the ground multiplet of (2, 3) will transform as an irreducible representation $\tilde{\Upsilon}$ of the group. The generators in that representation (the "new spin" operators) will be denoted by $\tilde{\mathbf{L}}$. Since the SDRG must preserve the global symmetry, the effective Hamiltonian reads

$$\tilde{\mathcal{H}} = \sum_{\Upsilon} \tilde{K}_1^{\Upsilon} \mathcal{O}^{\Upsilon}(\mathbf{L}_1, \tilde{\mathbf{L}}) + \sum_{\Lambda} \tilde{K}_3^{\Upsilon} \mathcal{O}^{\Upsilon}(\tilde{\mathbf{L}}, \mathbf{L}_4). \tag{26}$$

The challenge here is to find the renormalized couplings $\tilde{K}_i^{\Upsilon}$. According to (10), we need the matrix elements of $T_{\lambda}^{\Upsilon}(\mathbf{L}_i)$

($i = 2, 3$) within the $\tilde{\Upsilon}$ space. Using the Wigner-Eckart theorem in Eq. (23) twice, for both the matrix elements of $T_{\upsilon}^{\Upsilon}(\mathbf{L}_i)$ ($i = 2, 3$) and $T_{\upsilon}^{\Upsilon}(\tilde{\mathbf{L}})$, one finds

$$\langle \tilde{\Upsilon} \upsilon_1 | T_{\upsilon}^{\Upsilon}(\mathbf{L}_i) | \tilde{\Upsilon} \upsilon_2 \rangle$$
$$= \langle \tilde{\Upsilon} \upsilon_1 | \Upsilon \upsilon \tilde{\Upsilon} \upsilon_2 \rangle \langle \Upsilon_2 \Upsilon_3; \tilde{\Upsilon} \| T^{\Upsilon}(\mathbf{L}_i) \| \Upsilon_2 \Upsilon_3; \tilde{\Upsilon} \rangle, \tag{27}$$

$$\langle \tilde{\Upsilon} \upsilon_1 | T_{\upsilon}^{\Upsilon}(\tilde{\mathbf{L}}) | \tilde{\Upsilon} \upsilon_2 \rangle$$
$$= \langle \tilde{\Upsilon} \upsilon_1 | \Upsilon \upsilon \tilde{\Upsilon} \upsilon_2 \rangle \langle \Upsilon_2 \Upsilon_3; \tilde{\Upsilon} \| T^{\Upsilon}(\tilde{\mathbf{L}}) \| \Upsilon_2 \Upsilon_3; \tilde{\Upsilon} \rangle. \tag{28}$$

As long as the Clebsch-Gordan coefficients are nonzero, we can divide these equations, and use the fact we are within the subspace of fixed $\tilde{\Upsilon}$ (i.e., the local ground multiplet), to obtain the following operator identity within the $\tilde{\Upsilon}$ representation:

$$T_{\upsilon}^{\Upsilon}(\mathbf{L}_i) = \frac{\langle \Upsilon_2 \Upsilon_3; \tilde{\Upsilon} \| T^{\Upsilon}(\mathbf{L}_i) \| \Upsilon_2 \Upsilon_3; \tilde{\Upsilon} \rangle}{\langle \Upsilon_2 \Upsilon_3; \tilde{\Upsilon} \| T^{\Upsilon}(\tilde{\mathbf{L}}) \| \Upsilon_2 \Upsilon_3; \tilde{\Upsilon} \rangle} T_{\upsilon}^{\Upsilon}(\tilde{\mathbf{L}}) \tag{29}$$

$$\equiv \beta_i(\Upsilon, \tilde{\Upsilon}, \Upsilon_2, \Upsilon_3) T_{\upsilon}^{\Upsilon}(\tilde{\mathbf{L}}), \quad i = 2, 3. \tag{30}$$

Comparing with Eq. (26), the couplings are corrected by

$$\tilde{K}_i^{(\Upsilon)} = \beta_i(\Upsilon, \tilde{\Upsilon}, \Upsilon_2, \Upsilon_3) K_i^{(\Upsilon)}, \quad i = 1, 3, \tag{31}$$

controlled uniquely by the reduced matrix elements of the tensor operators within the ground-state multiplet representation. The value of the Wigner-Eckart theorem cannot be overstated here: it guarantees both that the renormalized Hamiltonian remains written in terms of only scalar operators and that distinct ranks are not mixed.

First-order perturbation theory fails whenever the right-hand sides of Eqs. (27) and (28) vanish. For concreteness, focus on Eq. (27). Two cases arise for which the coefficient vanishes:

(i) When $\tilde{\Upsilon} \notin \Upsilon \otimes \tilde{\Upsilon}$. In this case the very Clebsch-Gordan coefficients $\langle \tilde{\Upsilon} \upsilon_1 | \Upsilon \upsilon \tilde{\Upsilon} \upsilon_2 \rangle$ vanish. This case is the easiest to predict, since it comes directly from the Clebsch-Gordan series of the group and does not rely on dynamics.

(ii) When $\tilde{\Upsilon} \in \tilde{\Upsilon} \otimes \Upsilon$, but $\langle \Upsilon_2 \Upsilon_3; \tilde{\Upsilon} \| T^{\Upsilon}(\mathbf{L}_i) \| \Upsilon_2 \Upsilon_3; \tilde{\Upsilon} \rangle$ is still zero. This is a more exotic scenario, but is present even in the more familiar SU(2) problem [17]. Since there is no (easy) way to predict when this happens *a priori*, one has to compute such reduced matrix element explicitly to find out whether it is zero or not.

Case (i) happens whenever the ground state is a singlet. This is a natural situation and leads us to deal with the problem within second-order perturbation theory, as explained in the next subsection. In any other situation in which one of the cases listed above happens, the neighboring couplings are immediately renormalized to zero and the SDRG flow, as derived here, becomes pathological. Dealing with this situation would require going to the next order in perturbation theory, and in general, as exemplified in Ref. [17], the form of the Hamiltonian is not maintained. This complicates considerably the analysis. As we show later, case (i) happens in a region of the Sp(N) antiferromagnetic phase diagram. The SO(N) Hamiltonian, however, is protected against such anomalies by the location of SU(N)-symmetric points in its phase diagram. This will become evident in next sections, as we explicitly compute the prefactors for the SO(N) case.

B. Second-order perturbation theory

We return to the 4-site chain, now with the assumption that the most strongly coupled sites 2 and 3 have a singlet ground state. The singlet ground state is trivial, in the sense of having no dynamics, and no effective spin remains. This situation causes the first-order perturbation theory to vanish, as described above, and we have to rework the effective problem to second order in perturbation theory. The 4-site problem becomes a two-site problem with site 1 effectively coupled to 4 (see Fig. 3).

We call the singlet state $|s\rangle$ and we call $\mathcal{H}^{(2)}_{\Upsilon,\Upsilon'}$ the effective Hamiltonian connecting sites 1 and 4 coming from tensors of rank Υ and Υ'. By standard second-order perturbation theory, $\mathcal{H}^{(2)}_{\Upsilon,\Upsilon'}$ reads

$$\mathcal{H}^{(2)}_{\Upsilon,\Upsilon'} = 2K_1^{\Upsilon} K_3^{\Upsilon'} \sum_{\upsilon,\upsilon'} T_\upsilon^{\Upsilon}(\mathbf{L}_1) \Delta \mathcal{H}^{\Upsilon\Upsilon'}_{\upsilon,\upsilon'} T_{\upsilon'}^{\Upsilon'}(\mathbf{L}_4), \quad (32)$$

where

$$\Delta \mathcal{H}^{\Upsilon\Upsilon'}_{\upsilon,\upsilon'} = \sum_{\tilde{\Upsilon},\tilde{\upsilon}} \frac{\langle s|T_\upsilon^{\Upsilon}(\mathbf{L}_2)|\tilde{\Upsilon}\tilde{\upsilon}\rangle \langle \tilde{\Upsilon}\tilde{\upsilon}|T_{\upsilon'}^{\Upsilon'}(\mathbf{L}_3)|s\rangle}{\Delta E_{\tilde{\Upsilon}}(\mathbf{L}_2,\mathbf{L}_3)}. \quad (33)$$

The sum over $\tilde{\Upsilon}$ is over all representations arising from the Clebsch-Gordan series of $\mathbf{L}_2 \otimes \mathbf{L}_3$, excluding the singlet. The energy denominator $\Delta E_{\tilde{\Upsilon}}$ is the difference between the energies of the singlet and that of the multiplet $\tilde{\Upsilon}$.

The main goal is to simplify Eq. (33) using all the selection rules available. Again, from Eq. (23),

$$\langle s|T_\upsilon^{\Upsilon}(\mathbf{L}_2)|\tilde{\Upsilon}\tilde{\upsilon}\rangle$$
$$= \langle \Upsilon\tilde{\Upsilon}, s|\Upsilon\upsilon\tilde{\Upsilon}\tilde{\upsilon}\rangle \langle \Upsilon\|T_\upsilon^{\Upsilon}(\mathbf{L}_2)\|\tilde{\Upsilon}\rangle. \quad (34)$$

The coefficient $\langle \Upsilon\tilde{\Upsilon}, s|\Upsilon\upsilon\tilde{\Upsilon}\tilde{\upsilon}\rangle$ is nonvanishing only if the representations Υ and $\tilde{\Upsilon}$ have a singlet in their Clebsch-Gordan series. In this case, they are called mutually complementary. For every Lie algebra, given a representation Υ, only one other unique representation $\tilde{\Upsilon}$ exists that is complementary to it [29]. For so(N) and sp(N) algebras, every representation is complementary to itself, $\tilde{\Upsilon} = \Upsilon$. For the other cases, the complementary to a given representation, though not necessarily equal to it, has the same dimension. In su(N), for instance, the fundamental and antifundamental representations generate singlets when combined. Therefore, the sum over $\tilde{\Upsilon}$ is reduced to the single complementary representation $\tilde{\Upsilon}$. Applying this analysis to the matrix element of the tensor living on site 3, $T_{\upsilon'}^{\Upsilon'}(\mathbf{L}_3)$, we arrive at the selection rule $\Upsilon' = \tilde{\Upsilon}$. Thus,

$$\Delta \mathcal{H}^{\Upsilon\Upsilon'}_{\upsilon,\upsilon'} = \delta_{\Upsilon',\tilde{\Upsilon}} \sum_{\tilde{\upsilon}} \frac{\langle s|T_\upsilon^{\Upsilon}(\mathbf{L}_2)|\tilde{\Upsilon}\tilde{\upsilon}\rangle \langle \tilde{\Upsilon}\tilde{\upsilon}|T_{\upsilon'}^{\tilde{\Upsilon}}(\mathbf{L}_3)|s\rangle}{\Delta E_{\tilde{\Upsilon}}(\mathbf{L}_2,\mathbf{L}_3)}$$
$$= \delta_{\Upsilon',\Upsilon} \frac{\sum_{\tilde{\upsilon}} \langle s|T_\upsilon^{\Upsilon}(\mathbf{L}_2)|\Upsilon\tilde{\upsilon}\rangle \langle \Upsilon\tilde{\upsilon}|T_{\upsilon'}^{\Upsilon}(\mathbf{L}_3)|s\rangle}{\Delta E_{\Upsilon}(\mathbf{L}_2,\mathbf{L}_3)}, \quad (35)$$

where, in the second equality, we have used the identity $\sum_{\tilde{\Upsilon},\tilde{\upsilon}} |\tilde{\Upsilon}\tilde{\upsilon}\rangle\langle\tilde{\Upsilon}\tilde{\upsilon}| = \mathbf{1}$ and finally particularized the result to SO(N) and Sp(N) by using $\tilde{\Upsilon} = \Upsilon$.

Using the decomposition of the identity operator

$$\sum_{\tilde{\upsilon}} |\Upsilon\tilde{\upsilon}\rangle\langle\Upsilon\tilde{\upsilon}| = \mathbf{1} - \sum_{\tilde{\Upsilon}\neq\Upsilon,\tilde{\upsilon}} |\tilde{\Upsilon}\tilde{\upsilon}\rangle\langle\tilde{\Upsilon}\tilde{\upsilon}|, \quad (36)$$

and using $\langle \tilde{\Upsilon}\tilde{\upsilon}|T_\upsilon^{\Upsilon}(\mathbf{L}_{2,3})|s\rangle = 0$, for $\tilde{\Upsilon} \neq \Upsilon$, we obtain

$$\Delta \mathcal{H}^{\Upsilon\Upsilon'}_{\upsilon,\upsilon'} = \frac{\delta_{\Upsilon',\Upsilon}}{\Delta E_{\Upsilon}(\mathbf{L}_2,\mathbf{L}_3)} \langle s|T_{2,\upsilon}^{\Upsilon}(\mathbf{L}_2) T_{3,\upsilon'}^{\Upsilon}(\mathbf{L}_3)|s\rangle. \quad (37)$$

Now, from the symmetry properties of the Hamiltonian, preserved by the SDRG, the effective Hamiltonian must read

$$\tilde{\mathcal{H}} \propto \mathcal{O}^{\Upsilon}(\mathbf{L}_1,\mathbf{L}_4), \quad (38)$$

since this is the only symmetric scalar operator that can be built out of Υ-rank tensors. The remaining matrix element can thus be computed to give [29]

$$\langle s|T_{2,\upsilon}^{\Upsilon}(\mathbf{L}_2) T_{3,\upsilon'}^{\Upsilon}(\mathbf{L}_3)|s\rangle = \delta_{\upsilon',-\upsilon}(-1)^{f(\Upsilon,\upsilon)}\alpha(\Upsilon,\mathbf{L}_2,\mathbf{L}_3), \quad (39)$$

where $\alpha(\Upsilon,\mathbf{L}_2,\mathbf{L}_3)$, the reduced matrix element, is a function of the tensor rank Υ and the spins being decimated. Its explicit value will be determined for the cases of interest. Collecting the results and plugging them back into Eq. (32), we arrive at the effective Hamiltonian connecting sites 1 and 4,

$$\mathcal{H}^{(2)}_{\Upsilon,\Upsilon'} \equiv \frac{2\delta_{\Upsilon',\Upsilon}\alpha(\Upsilon,\mathbf{L}_2,\mathbf{L}_3)}{\Delta E_{\Upsilon}(\mathbf{L}_2,\mathbf{L}_3)} K_1^{\Upsilon} K_3^{\Upsilon}$$
$$\times \sum_{\upsilon} T_\upsilon^{\Upsilon}(\mathbf{L}_1)(-1)^{f(\Upsilon,\upsilon)} T_{-\upsilon}^{\Upsilon}(\mathbf{L}_4)$$
$$= \frac{2\delta_{\Upsilon',\Upsilon}\alpha(\Upsilon,\mathbf{L}_2,\mathbf{L}_3)}{\Delta E_{\Upsilon}(\mathbf{L}_2,\mathbf{L}_3)} K_1^{\Upsilon} K_3^{\Upsilon} \mathcal{O}^{\Upsilon}(\mathbf{L}_1,\mathbf{L}_4), \quad (40)$$

where in the last step we have used Eq. (10) to identify $\mathcal{O}^{\Upsilon}(\mathbf{L}_1,\mathbf{L}_4)$.

This derivation guarantees that tensors of different ranks again do not get mixed by the SDRG, which simplifies the analysis of the flow dramatically. In fact, this is the advantage of working with irreducible tensors [17]. Also, the functional form of the Hamiltonian does not change by the decimation steps. This is schematically represented in Fig. 3. Summing up, the coupling constants renormalize according to

$$\tilde{K}_{1,4}^{\Upsilon} = \frac{2\alpha(\Upsilon,\mathbf{L}_2,\mathbf{L}_3)}{\Delta E_{\Upsilon}(\mathbf{L}_2,\mathbf{L}_3)} K_1^{\Upsilon} K_3^{\Upsilon}. \quad (41)$$

This is the generalization to any symmetry group of the SDRG step first derived for SU(2)-symmetric spin-1/2 chains in Refs. [21,22] and generalized to any SU(2) spin in Ref. [38].

The application of the SDRG has thus been generalized for spin chains of any Lie group symmetry. The main ingredients for this are the identification of the tensor operator technology, and the Wigner-Eckart theorem. In what follows, we apply the formulas to the SO(N) and Sp(N) cases of our interest, finding closed expressions for the prefactors.

C. SO(N) rules in closed form

Let us particularize Eqs. (31) and (41), which dictate how the couplings are renormalized in SDRG steps, to the case of SO(N)-symmetric Hamiltonians. To do so, we start with Eq. (17) for the strongly coupled sites 2 and 3:

$$\mathcal{H}_{2,3} = K_2^{(1)} \mathcal{O}^{(1)}(\mathbf{L}_2,\mathbf{L}_3) + K_2^{(2)} \mathcal{O}^{(2)}(\mathbf{L}_2,\mathbf{L}_3). \quad (42)$$

In what follows, it proves useful to rewrite the two coupling constants of each bond $(K_i^{(1)}, K_i^{(2)})$ in polar coordinates. In

particular, as we will see, the ratio of Eqs. (31) and (41) fully controls the renormalization of the angles θ_i,

$$\tan \theta_i = \frac{K_i^{(2)}}{K_i^{(1)}}, \tag{43}$$

while the radial variable

$$r_i = \sqrt{\left(K_i^{(1)}\right)^2 + \left(K_i^{(2)}\right)^2} \tag{44}$$

controls the energy scale.

It will be important for our later discussion to know that some points of the parameter space have, in fact, SU(N) symmetry. First, $K_i^{(1)} = K_i^{(2)}$ is an obvious SU(N)-symmetric point, where the Hamiltonian becomes

$$\mathcal{H}_{2,3} = K_2^{(1)} \sum_{\mu=1}^{N^2-1} \Lambda_2^\mu \Lambda_3^\mu, \tag{45}$$

which is the Heisenberg SU(N) Hamiltonian at sites (2, 3). This corresponds to the $\theta = \frac{\pi}{4}$ point in the polar coordinates of Eq. (43).

The choice $K_i^{(1)} = -K_i^{(2)}$ is also SU(N) symmetric ($\theta = -\frac{\pi}{4}$). This can be shown in the following way. Starting from the SU(N)-invariant point $\theta = \frac{\pi}{4}$, we transform all SU(N) generators as $\Lambda_i^a \to -\Lambda_i^{a*}$ on every other site. This changes the corresponding SU(N) representation from the fundamental to the antifundamental, which is its complex conjugate. To show the SU(N) invariance, recall that $\mathcal{O}^{(1)}$ is built with the generators of SO(N), which are purely imaginary antisymmetric objects and, therefore, do not change sign under this transformation. Meanwhile, all the terms in $\mathcal{O}^{(2)}$ are constructed using the real generators of SU(N) and will, therefore, flip sign. By absorbing this sign change into $K_i^{(2)}$, we see that the point $\theta = -\frac{\pi}{4}$ is also SU(N) symmetric.

Notice that the derivation of the last section guarantees that no operators other than $\mathcal{O}^{(1)}$ and $\mathcal{O}^{(2)}$ will be generated during the RG flow. This would not have been obvious had we not been aware that the SU(N) anisotropy keeps the underlying SO(N) structure intact. We will, in what follows, make full use of the fact that the SO(N)-symmetric Hamiltonian can be thought of as an anisotropic SU(N) Hamiltonian and also that the renormalization prefactors are determined by very few quantities: (i) the representations Υ_2 and Υ_3 of spins on sites 2 and 3, and (ii) the two-spin ground manifold $\tilde{\Upsilon}$.

1. First-order perturbation theory

According to Eqs. (31), for both links 1 and 3, the renormalization of $\tan \theta_i$ (the ratio of couplings) is given by

$$\tan \tilde{\theta}_{1,3} = \frac{\beta_{1,3}(2, \tilde{\Upsilon}, \Upsilon_2, \Upsilon_3)}{\beta_{1,3}(1, \tilde{\Upsilon}, \Upsilon_2, \Upsilon_3)} \tan \theta_{1,3}. \tag{46}$$

To compute these we take a shortcut using the results of Sec. III A. Since the SDRG preserves the SU(N) symmetry, we expect that if we start with all angles equal to $\frac{\pi}{4}$, $\tilde{\theta}$ has to be equal to $\pm\frac{\pi}{4}$. From that, we find that the only possible values for the ratios of $\tan \tilde{\theta}_{1,3} / \tan \theta_{1,3}$ are ± 1, with the sign depending on the representations. At this stage, we parametrize

$$\tilde{K}_{1,3}^{(1)} = \Phi_{1,3} K_{1,3}^{(1)}, \tag{47}$$

TABLE III. List of the prefactors ξ_1, ξ_3, Φ_1, and Φ_3 used in the first-order decimations.

	ξ_1	ξ_3	Φ_1	Φ_3
$\tilde{Q} = Q_2 + Q_3$ and $Q_2 + Q_3 \leqslant \mathrm{int}(\frac{N}{2})$	1	1	$\frac{Q_2}{Q_2 + Q_3}$	$\frac{Q_3}{Q_2 + Q_3}$
$\tilde{Q} = N - (Q_2 + Q_3)$ and $Q_2 + Q_3 > \mathrm{int}(\frac{N}{2})$	-1	-1	$\frac{Q_2}{Q_2 + Q_3}$	$\frac{Q_3}{Q_2 + Q_3}$
$\tilde{Q} = \lvert Q_3 - Q_2 \rvert$	-1	1	$\frac{Q_2}{N - Q_2 + Q_3}$	$\frac{N - Q_3}{N - Q_2 + Q_3}$

$$\tilde{K}_{1,3}^{(2)} = \Phi_{1,3} \xi_{1,3} K_{1,3}^{(2)}, \tag{48}$$

with $\xi_{1,3}(\tilde{\Upsilon}, \Upsilon_2, \Upsilon_3) = \pm 1$ and $\Phi_{1,3}(\tilde{\Upsilon}, \Upsilon_2, \Upsilon_3)$ to be determined according to the representations.

In order to determine ξ and Φ, we identify the representations Υ in a Young-tableau notation for SO(N). Since we focus on the phase in which only antisymmetric representations are generated by the SDRG flow, we specify them by Q, the number of vertically concatenated boxes. We also chose for concreteness $Q_2 \leqslant Q_3$ and assume that the two-spin ground state $\tilde{Q}$ is not a singlet, so that first-order renormalization is required. All possible relevant cases are listed in Table III, with the values of ξ and Φ provided. In general, sign flips always happen on the bond on the side of the smaller Q_i ($i = 2, 3$) of the decimated pair. The derivation of the values of ξ_1, ξ_3, Φ_1, and Φ_3 is given in the Appendix.

2. Second-order perturbation theory

Particularizing the second-order SDRG decimation derived in Sec. IV B to SO(N), the effective Hamiltonian between sites 1 and 4 acquires the following form:

$$\Delta \mathcal{H}_{(1,4)}^{(2)} = \tilde{K}_{1,4}^{(1)} \mathcal{O}^{(1)}(\mathbf{L}_1, \mathbf{L}_4) + \tilde{K}_{1,4}^{(2)} \mathcal{O}^{(2)}(\mathbf{L}_1, \mathbf{L}_4). \tag{49}$$

Going back to Eq. (41), we can write explicitly

$$\tilde{K}_{1,4}^{(1)} = \alpha^{(1)}(\mathbf{L}_2, \mathbf{L}_3) \frac{K_1^{(1)} K_3^{(1)}}{E_{[0,0]} - E_{[1,1]}}, \tag{50}$$

$$\tilde{K}_{1,4}^{(2)} = \alpha^{(2)}(\mathbf{L}_2, \mathbf{L}_3) \frac{K_1^{(2)} K_3^{(2)}}{E_{[0,0]} - E_{[2,0]}}, \tag{51}$$

with $\alpha^{(1,2)}$ yet to be determined. The energies in the denominators come from the spectrum of the strongly coupled pair of sites (2, 3), Eq. (42). $E_{[0,0]}$ is the energy of the singlet representation [0, 0], while the energies $E_{[1,1]}$ and $E_{[2,0]}$ correspond to the representations complementary to the ones of the operators forming the scalars $\mathcal{O}^{(1)}$ and $\mathcal{O}^{(2)}$, respectively. As pointed out before, for SO(N), these are just the same as the ranks of the scalars themselves.

A key observation is that the gaps $E_{[0,0]} - E_{[1,1]}$ and $E_{[0,0]} - E_{[2,0]}$ close at the point where the [0, 0] and [1, 1] representations cross, a generalization of the Affleck-Kennedy-Lieb-Tasaki (AKLT) point of the SU(2) spin-1 chain [39], and at the SU(N)-invariant points, respectively. Since the energy denominators are linear in $K_2^{(1)}$ and $K_2^{(2)}$, we must have

$$E_{[0,0]} - E_{[1,1]} \propto K_2^{(1)} (\tan \theta_{\mathrm{AKLT}(N)} - \tan \theta_2), \tag{52}$$

$$E_{[0,0]} - E_{[2,0]} \propto K_2^{(1)} (\tan \theta_{\mathrm{SU}(N)} - \tan \theta_2). \tag{53}$$

The generalized AKLT point is known for SO(N) systems to be given by [31]

$$\tan\theta_{\text{AKLT}(N)} = \frac{N-2}{N+2}, \quad (54)$$

while the SU(N)-symmetric point where the representations [0, 0] and [2, 0] meet in energy is antipodal to $\pi/4$,

$$\theta_{SU(N)} = -\frac{3\pi}{4}. \quad (55)$$

At this stage, the rules are simplified to

$$\tilde{K}_{1,4}^{(1)} = \tilde{\alpha}^{(1)}(\mathbf{L}_2, \mathbf{L}_3)\frac{K_1^{(1)}K_3^{(1)}}{K_2^{(1)}(\tan\theta_{\text{AKLT}(N)} - \tan\theta_2)}, \quad (56)$$

$$\tilde{K}_{1,4}^{(2)} = \tilde{\alpha}^{(2)}(\mathbf{L}_2, \mathbf{L}_3)\frac{K_1^{(2)}K_3^{(2)}}{K_2^{(1)}(1 - \tan\theta_2)}, \quad (57)$$

with the remaining task of determining the newly defined $\tilde{\alpha}^{(1,2)}$. For that, we can take advantage again of the presence of an SU(N)-symmetric point in the phase diagram. At the SU(N)-symmetric point $-\frac{\pi}{4}$, $K_i^{(1)} = -K_i^{(2)}$ and, once again enforcing that the SDRG must preserve the SU(N) symmetry, $\tilde{K}_{1,4}^{(1)} = -\tilde{K}_{1,4}^{(2)}$. Dividing Eqs. (56) and (57), we conclude that

$$\frac{\tilde{\alpha}^{(1)}(\mathbf{L}_2, \mathbf{L}_3)}{\tilde{\alpha}^{(2)}(\mathbf{L}_2, \mathbf{L}_3)} = -\frac{(\tan\theta_{\text{AKLT}(N)} + 1)}{2}. \quad (58)$$

Once the ratio is fixed, the value of $\tilde{\alpha}^{(2)}$ can be found by comparing Eq. (57) with the RG step for SU(N)-symmetric chains from Ref. [35],

$$\tilde{\alpha}^{(2)}(\mathbf{L}_2, \mathbf{L}_3) = -\frac{4Q(N-Q)}{N^2(N-1)}, \quad (59)$$

where $Q_2 = Q_3 = Q$ is the number of boxes in the Young tableaux of SO(N) at sites 2 and 3. Recall that a necessary condition for singlet formation is that the same representation appears on both sites. Putting everything together, we get

$$\tilde{K}_{1,4}^{(1)} = \left[\frac{4Q(N-Q)}{(N-1)N(N+2)}\right]\frac{K_1^{(1)}K_3^{(1)}}{K_2^{(1)}\left(\frac{N-2}{N+2} - \tan\theta_2\right)}, \quad (60)$$

$$\tilde{K}_{1,4}^{(2)} = -\left[\frac{4Q(N-Q)}{N^2(N-1)}\right]\frac{K_1^{(2)}K_3^{(2)}}{K_2^{(1)}(1 - \tan\theta_2)}. \quad (61)$$

The renormalization of the angle is found by dividing Eq. (60) by (61):

$$\tan\tilde{\theta}_{1,4} = -\left(\frac{N+2}{N}\right)\frac{\frac{N-2}{N+2} - \tan\theta_2}{1 - \tan\theta_2}\tan\theta_1\tan\theta_3. \quad (62)$$

One can verify explicitly from Eq. (62) the existence of *angular fixed points*. These points are such that

$$\tan\tilde{\theta}_{1,4} = \tan\theta_i, \quad i = 1, 2, 3. \quad (63)$$

Besides the SU(N)-symmetric point $\tan\theta_i = -1$ ($\theta_i = -\frac{\pi}{4}$), by using Eq. (62), we find that $\tan\theta_i = 0(\theta_i = 0)$ and $\tan\theta_i \to -\infty(\theta_i = -\frac{\pi}{2})$ are also angular fixed points. At this stage, we are also able to determine their stability. By including a perturbation $\delta\theta_i$ to the fixed points and by expanding Eq. (62) in powers of $\delta\theta$, we find that $\theta_i = 0$ and $\theta_i = -\frac{\pi}{2}$ are stable, whereas $\theta_i = -\frac{\pi}{4}$ is unstable. This is expected since they are SU(N)-symmetric points and deviations from this symmetry

are expected to be amplified by the SDRG. Notice that in this analysis we assume that only second-order decimation occurs, which can be achieved by the choice of the initial angle distribution, as we will show later. In the case where Eq. (62) leads also to first-order decimations, the representations will also flow, and the analysis of the angular fixed points as well as their stability is more elaborate. We postpone this analysis for later.

D. Sp(N) rules in closed form

The derivation of the Sp(N) rules is analogous to that for SO(N) in so far as only second-order decimations are present. We can again use the shortcut of having an SU(N)-symmetric point to explicitly compute the necessary prefactors. Just as in the SO(N) case, we work with polar coordinates with the angle θ_i defined as $\tan\theta_i = \frac{K_i^{(2)}}{K_i^{(1)}}$. These rules allow us to completely characterize the physics of a large fraction of the Sp(N) AF phase diagram and read

$$\tilde{K}_{1,4}^{(1)} = \left(\frac{4Q^2}{(N-1)N(N+2)}\right)\frac{K_1^{(1)}K_3^{(1)}}{K_2^{(1)}\left(\frac{N-2}{N+2} - \tan\theta_2\right)}, \quad (64)$$

$$\tilde{K}_{1,4}^{(2)} = -\left(\frac{4Q^2}{N^2(N-1)}\right)\frac{K_1^{(1)}K_3^{(1)}}{K_2^{(1)}(1 - \tan\theta_2)}, \quad (65)$$

where Q denotes the number of boxes in the Sp(N) Young tableaux at sites 2 and 3.

The situation is different, however, when first-order decimations in the AF region are also required. The reason is that this region has no SU(N)-symmetric point. This implies that the above shortcut of using these points to compute the prefactors is no longer valid. We can, however, build the Sp(N) tensors explicitly, and from that, calculate all the necessary prefactors. We will come back to this point when we study the Sp(N) SDRG flow.

V. THE PHASE DIAGRAM OF STRONGLY DISORDERED SO(N) AND Sp(N) SPIN CHAINS

With the decimation rules of the previous section, we are now able to characterize the SDRG flow for SO(N) and Sp(N) chains. The characterization of the RG flow involves finding the low-energy behavior of the joint distribution of θ, r, and the representations Υ at energy scale Ω, $P(r, \theta, \Upsilon; \Omega)$. At the beginning of the flow we set $\Omega = \Omega_0$ and assume a distribution without any correlations between different sites. Furthermore, we take the initial distribution to be separable, $P(r, \theta, \Upsilon; \Omega_0) = P_r(r)P_\theta(\theta)P_\Upsilon(\Upsilon)$, with the angular part taken to be a delta function,

$$P_\theta(\theta) = \delta(\theta - \theta_0). \quad (66)$$

The assumption of such an initial distribution simplifies the analysis of the SDRG flow dramatically. This polar parametrization was first introduced in Ref. [20] in the context of spin-1 chains, equivalent to the SO(3) case discussed in this paper. Allowing the initial angular distribution to have a nonzero broadness σ_θ makes the analysis of the SDRG flow more intricate. The low-energy phase depends in a complicated manner on θ_0 and σ_θ (see Fig. 1 and the corresponding
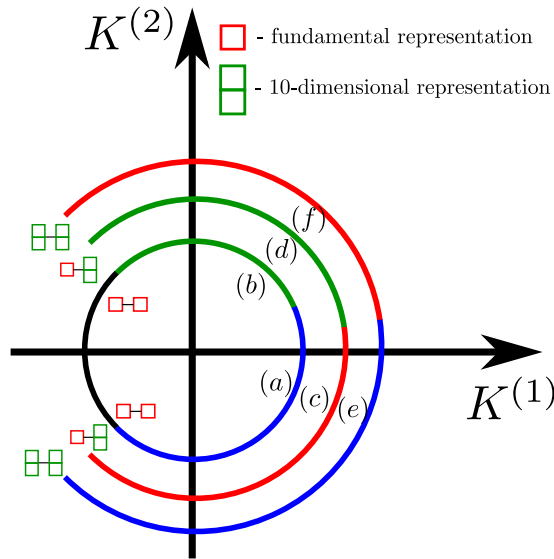
FIG. 4. Ground-state structure of the SO(5) two-site problem as a function of the angle θ, with different colors representing the distinct multiplets. Each arc of fixed radius corresponds to the ground-state multiplets for the two representations indicated next to it by Young tableaux. The singlet state is represented in blue, the fundamental 5-dimensional [1, 0] multiplet in red [represented by a single box, in SO(N) Young-tableau notation], and the 10-dimensional [1, 1] multiplet in green (represented by two boxes concatenated vertically). All other multiplets are colored black, and do not participate in the flow of antiferromagnetic phases. The points with $K^{(1)} > 0$ where there is a change in the ground state are generally called θ_{AKLT}. The other points where there is a change in the ground state for $K^{(1)} < 0$ are $\pm 3\pi/4$ [for any pair of SO(5) representations displayed]. The RG rules corresponding to the letters (a)–(f) are given in Fig. 5.

discussion in Ref. [20] for the spin-1 chain). Besides, other phases also appear, such as the so-called large spin phase (LSP) [38], whose physics goes beyond the scope of this paper. The determination of the complete phase diagram for finite σ_θ (with the exception of the LPSs) poses no additional difficulty and will not be done here.

Similarly, the initial choice of representations is not random but fixed at the defining representation, as mentioned previously,

$$P_\Upsilon(\Upsilon) = \delta(\Upsilon - [1, \vec{0}]). \qquad (67)$$

This is a possible choice that guarantees that only a finite number of representations are generated throughout the SDRG flow. Other choices can generically lead to arbitrarily larger representations. In contrast to $P_\theta(\theta)$ and $P_\Upsilon(\Upsilon)$, initial randomness is taken to be present in the radial variable r, through a finite standard deviation for $P_r(r)$. We also assume that this initial disorder distribution width is sufficiently large for the SDRG method to be applicable.

Let us now list some universal features of the SDRG flow in the antiferromagnetic (AF) phases [40]. During the initial stages of the flow, the distributions of angles, radii, and representations become correlated, but eventually become again uncorrelated at low energies $\Omega \ll \Omega_0$. Furthermore, at low energies, all angles tend to a single value; that is, P_θ flows back to a delta function centered at one of the angular

fixed points. This is the main advantage of parametrizing the SDRG flow using polar coordinates [20]. As for the radial distribution, it will flow at low energies to an infinite-disorder profile; that is, its standard deviation divided by its average diverges. More specifically [3,21,22],

$$P_r(r) \to \frac{1}{r^{1-\alpha}}, \quad \alpha^{-1} \sim \ln\left(\frac{\Omega_0}{\Omega}\right). \qquad (68)$$

In the phases discussed in this work, only antisymmetric representations are generated and the number of such distinct representations is finite. The frequency of distinct representations at low energies depends on N and on the region of the parameter space.

At low energies, the remaining nondecimated spins are embedded in a "soup" of randomly located singlets with a wide distribution of sizes. At energy scale Ω, the average separation of nondecimated spins scales as $L_\Omega \sim |\ln \Omega|^{1/\psi}$, with the exponent ψ depending on the number of distinct representations at the low-energy fixed point [7,35]. At a scale $\Omega \sim T$, only nondecimated spins contribute to the susceptibility. Since the distributions of couplings is extremely broad, the spins will be typically very weakly coupled $r \ll T$. Thus, the susceptibility is given by Curie's law: $\chi(T)^{-1} \sim T L_T \sim T |\ln T|^{1/\psi}$ [3,27]. Other thermodynamic quantities follow from similar reasoning: the entropy density is $s(T) \sim (\ln N)/L_T$ and the specific heat $c(T) = T(ds/dT) \sim |\ln T|^{-1-1/\psi}$.

The ground state consists of singlets formed with all representations. These singlets are formed at various stages of the SDRG. On average, their sizes and strengths reflect the stage at which they were formed. Therefore, singlets coupled with strength r (i.e., whose higher multiplets are excited at this energy cost) have sizes $L_r \sim |\ln r|^{1/\psi}$. This picture motivates the name "random singlet phase" (RSP) [3,5,35].

In what follows, we add more detail to the above general picture and determine the phase diagrams of SO(N)-symmetric disordered chains. We do so separately for the cases of odd and even N as their analyses are different. Moreover, a more illuminating route consists of considering specific small values of N first and then generalizing to the larger ones. SO(2)-invariant Hamiltonians, obtained by including anisotropy terms in SU(2) Hamiltonians (i.e., the XXZ model), were first studied by Fisher [3]. Generic SO(3) Hamiltonians were studied more recently [20], in the context of spin-1 SU(2)-invariant Hamiltonians. Thus, we use the SDRG flows of the groups SO(4) and SO(5) as the simplest yet unexplored examples of orthogonal symmetric Hamiltonians. Then, the extrapolation to arbitrary N is found to be straightforward. The $N = 4$ case presents a feature that is not present for any other N, which makes the construction of its phase diagram slightly more subtle. For this reason, we will take up the odd-N case first. For symplectic-invariant Hamiltonians, we are not aware of any previous analysis via the SDRG. We focus on discussions of Sp(4) and Sp(6), and provide a brief analysis and expectations for larger N.

A. SO(N) for odd values of N

To begin the analysis of odd-N SO(N)-symmetric disordered chains, we focus first on SO(5). In Fig. 4, we represent the ground states of the two-spin problems as functions of θ
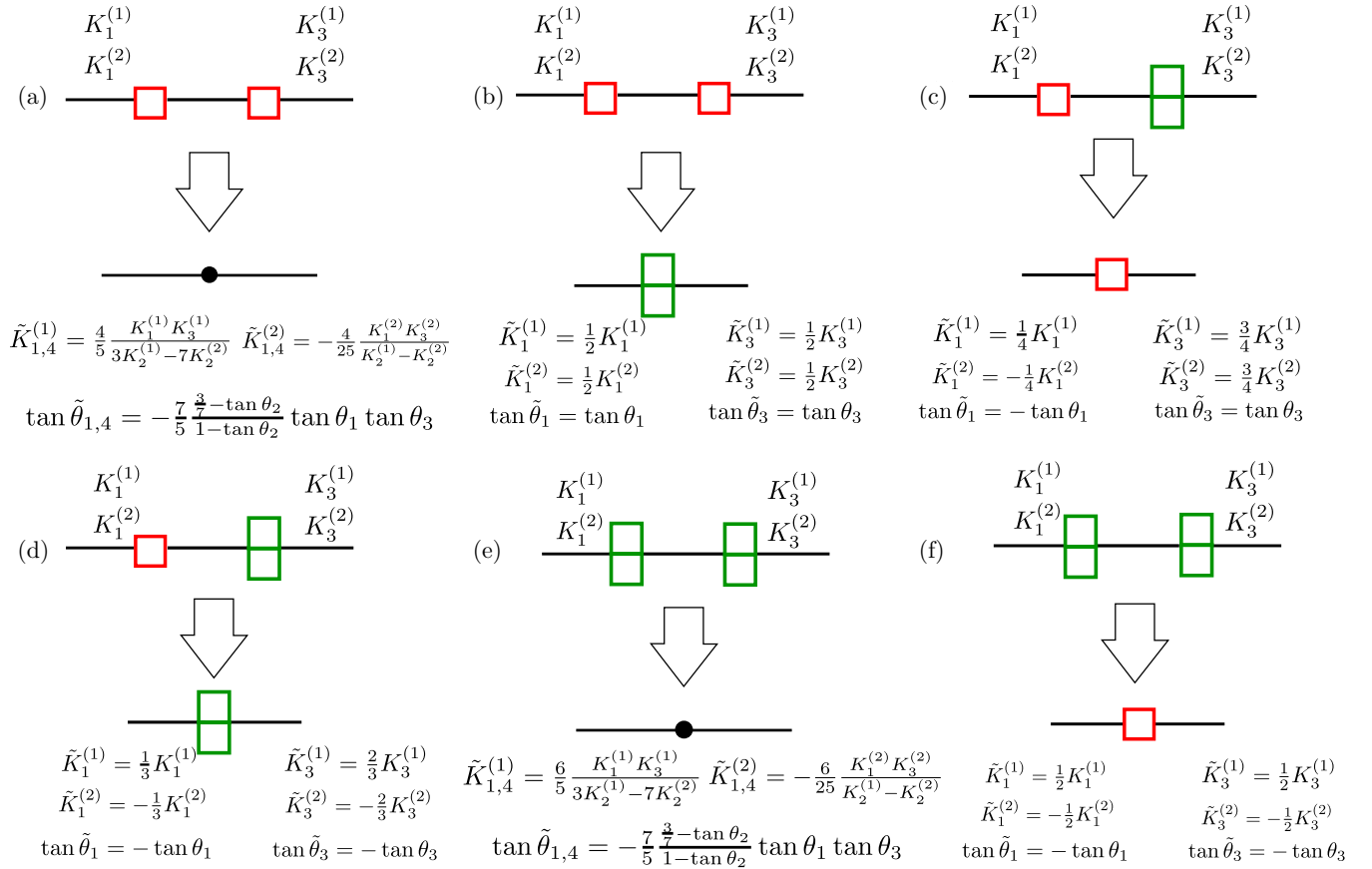
FIG. 5. All possible decimations and RG rules needed for the antiferromagnetic phases of the SO(5) model, representing using the Young-tableau notation.

using a color code. The important representations and their respective colors for the AF SDRG flow are the singlet [0, 0] (blue), the fundamental [1, 0] (red), and [1, 1] (green). As discussed, the nontrivial ones have dimensions $d_{[1,0]} = 5$ and $d_{[1,1]} = 10$ and, in a Young-tableau language, are represented by a single box and by two vertically stacked boxes, respectively. Each circle represents a particular combination of representations for the two spins that are coupled, as indicated by the pair of Young tableaux next to it. The colors of the arcs of each circle indicate, through the color code, to which representation the ground multiplet belongs.

The innermost circle in Fig. 4 displays the possible ground states when the two spins are in the fundamental (defining) representation. The points where colors change, and so does the two-spin problem ground multiplet, are $-3\pi/4$, $3\pi/4$, for $K^{(1)} < 0$, and the angle $\theta_{\text{AKLT}(N=5)} = \arctan(3/7)$ [see Eq. (54)], for $K^{(1)} > 0$. We see that there are three possible representations for the ground multiplet: the totally symmetric, 14-dimensional [2, 0] (black), the [0, 0] singlet (blue), and the [1, 1] (green). Since in this work we do not focus on symmetric representations [analogous to the formation of "large spins" in the SU(2) case], we will neglect decimations in the black region. If a decimation in the chain is performed in the blue region, the two fundamental representation spins are substituted by a singlet and the neighboring couplings are renormalized in second order of perturbation theory. If a decimation is made in the green region, on the other hand,

the two [1, 0] spins are substituted by a single spin in the 10-dimensional [1, 1] representation and the renormalization of couplings is given by first-order perturbation theory. This representation, at a later point of the RG flow, will be decimated either with another fundamental [1, 0] object or with another [1, 1] object. This is why we need the other circles in Fig. 4. For SO(5), the relevant Clebsch-Gordan series are, therefore [34],

$$[1, 0] \otimes [1, 0] = \mathbf{[0, 0]} \oplus \mathbf{[1, 1]} \oplus [2, 0], \qquad (69)$$

$$[1, 0] \otimes [1, 1] = \mathbf{[1, 0]} \oplus \mathbf{[1, 1]} \oplus [2, 1], \qquad (70)$$

$$[1, 1] \otimes [1, 1] = \mathbf{[0, 0]} \oplus \mathbf{[1, 0]} \oplus [1, 1]$$
$$\oplus [2, 0] \oplus [2, 1] \oplus [2, 1]. \qquad (71)$$

The bold terms on the right-hand side are the relevant ones for the AF SDRG flow. For concreteness, we give in Fig. 5 all the RG rules for AF decimations in SO(5). By combining Fig. 4 and Fig. 5, we can characterize the SO(5) RG flow, as we explain next.

The initial condition of starting with the fundamental representation of SO(5) implies that the initial two-site ground-state structure relevant to us is the one in the innermost arc of Fig. 4. Two possibilities follow next, depending on what the initial angle θ_0 is. If the angle θ_0 is restricted to the blue region of Fig. 4 ($-\frac{3}{4}\pi < \theta_0 < \theta_{\text{AKLT}(N)}$), only singlets are
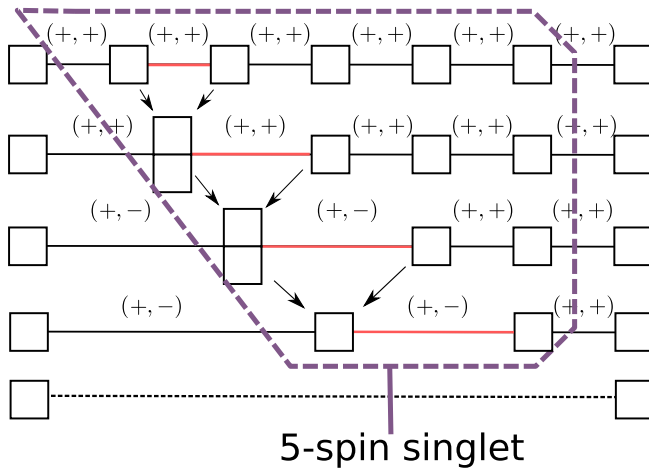
FIG. 6. From top to bottom, a possible decimation route leading to a 5-site singlet in an SO(5) chain. In red, we highlight the bond that is being decimated at a given step. Above each bond is the sign of its respective couplings $K_i^{(1)}$ and $K_i^{(2)}$. More than the numeric renormalization of the constants, the sign flips are crucial to follow the representation flow. In this example the net result of the first three steps is to flip a sign of one of the couplings, such that the pair of fundamental representations forms a singlet ground state in the last step.

formed throughout the flow [only decimation (a) in Fig. 5 happens]. This is because the renormalized angles also lie within the same blue range, as one can explicitly verify using the angular equation in Fig. 5(a). The distribution of angles has, therefore, to flow to one of the possible fixed points found in Sec. IV C 2. Since the SU(N)-symmetric angular fixed point $-\frac{\pi}{4}$ is unstable, the angular distribution remains there only if $\theta_0 = -\frac{\pi}{4}$. In all other cases, the angular distribution flows to either $\theta = -\pi/2$ or 0, depending on the initial value of θ_0. For $-3\pi/4 < \theta_0 < -\pi/4$, the flow is toward $\theta = -\pi/2$, whereas angles in the complementary region flow toward $\theta = 0$. Singlets are formed throughout the chain, with spins paired two-by-two, but with otherwise randomly distributed positions and sizes. Extending the conventions of the spin-1 chain [20], we will name this a "mesonic" phase.

In contrast to the case above, if the initial angle lies in the region $\theta_{\text{AKLT}(N)} < \theta_0 < \frac{3\pi}{4}$, first-order decimations will happen and the distribution of group representations will also flow. This is analogous to what happens in the SDRG flow when the couplings are random in sign in Heisenberg SU(2) spin chains, with the important difference that here only a few representations will enter the flow. As a consequence of the limited number of representations, we are guaranteed to obtain a singlet after a finite number of steps. The remaining question is what is the character of the ground state as well as of its low-lying excitations? The answer is that the ground state is formed by a collection of singlets formed by $N = 5$ or any integer multiple of 5 spins. One possible decimation route is exemplified in Fig. 6, for a five-spin singlet. In this figure, we show explicitly the signs of the couplings $(K_i^{(1)}, K_i^{(2)})$ of each bond. In each decimation, Fig. 5 has been used to determine whether the signs of neighboring bonds change or remain the same. Other cases can be worked at will, all of them yielding
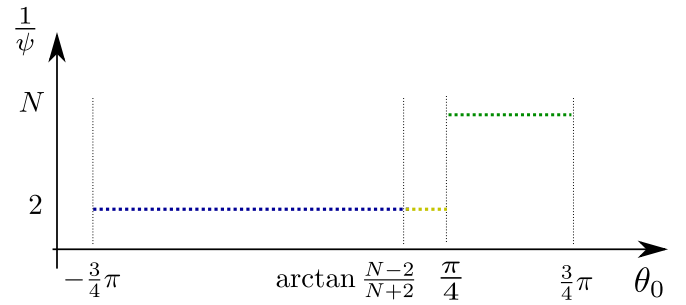
(integer $\times$ 5)-site singlets. This phase will be called here a "baryonic" phase [20].

To characterize the mesonic and baryonic phases thermodynamically, we have to determine the exponent ψ. For that, one first notices that only two types of decimation processes occur, those of first or second order. The analysis was carried out in Refs. [7,35] and will not be repeated here. Briefly, in the limit of wide distributions, the numerical prefactors of the renormalized couplings can be safely neglected. As a result, because of the multiplicative structure of Eq. (41), only second-order decimations are effective at lowering the energy scale. It follows that if asymptotically p is the fraction of second-order decimations, then

$$\psi = \frac{1}{1 + \frac{1}{p}}. \tag{72}$$

In the mesonic phase, there are only second-order processes so $p = 1$ and $\psi_M = 1/2$. On the other hand, in the baryonic phase, $p = 1/4$ and $\psi_B = 1/5$.

The SO(5) case can now be extrapolated to SO(N) for any odd value of N, as we have carefully checked numerically for the lowest odd-N values. The RG structure is very similar, with the only mentioned difference that the number of representations involved, in addition to the singlet, is larger. Thus, the ground state for SO(N), odd N, will be a collection of singlets made of either pairs of spins (mesonic phase) or multiples of N spins (baryonic phase). The mesonic phase is characterized by $\psi_M = 1/2$, as only second-order processes occur. In contrast, in the baryonic phase, the asymptotic probability of the latter processes is $p = 1/(N - 1)$ and thus $\psi_B = 1/N$ [7,35]. Figure 7 shows the value of the ψ exponent as a function of the initial angle θ_0. The mesonic phase is identified by the blue color whereas the baryonic one is green. The yellow region for $\arctan(\frac{N-2}{N+2}) < \theta_0 < \pi/4$ also belongs to the mesonic phase. As we will see next, the diagram is also valid for even values of N, although in that case the yellow region cannot be analyzed with the current approach.

B. SO(N) for even values of N

For even N, we start with SO(4). Even though it is the yet unexplored lowest-N case where our tools can be applied,

FIG. 7. Exponent ψ as a function of the initial angle θ_0, defined in Eq. (43), for SO(N)-symmetric Hamiltonians. The blue region is the mesonic phase whereas the green one is the baryonic phase. The yellow region $\theta_{\text{AKLT}(N)} < \theta_0 < \pi/4$ cannot be analyzed with the current method for even N, but should be regarded as blue (mesonic) for odd N.

TABLE IV. Spectrum of the most general SO(4) Hamiltonian following the convention of Eq. (73) (top) and Eq. (74) (bottom).

Degeneracy			E
1			$-3J + 9D$
3			$-J + D - 8F$
3			$-J + D + 8F$
9			$J + D$
Degeneracy	S_T	T_T	E
1	0	0	$-\frac{3}{4}(B_1 + B_2) + \frac{9}{16}B_{12} + B_0$
3	1	0	$\frac{1}{4}(B_1 - 3B_2) - \frac{3}{16}B_{12} + B_0$
3	0	1	$\frac{1}{4}(-3B_1 + B_2) - \frac{3}{16}B_{12} + B_0$
9	1	1	$\frac{1}{4}(B_1 + B_2) + \frac{1}{16}B_{12} + B_0$

it is very special because its Clebsch-Gordan series for the product of two fundamental representations has an additional term not present for any other value of N. As mentioned in connection with Eq. (11), the product of two fundamental representations of SO(N) generically yields three terms [29]. For SO(4), however, a fourth term is present. The proof of this statement can be found in Ref. [29]. The additional term in the Clebsch-Gordan series for SO(4) affects the form of the most generic Hamiltonian for a pair of spins. Specifically, for a pair of spins, one can have

$$\mathcal{H}_{SO(4)} = J\mathbf{L}_1 \cdot \mathbf{L}_2 + D(\mathbf{L}_1 \cdot \mathbf{L}_2)^2 + F\epsilon^{ijkl}L_1^{ij}L_2^{kl}, \quad (73)$$

where ϵ^{ijkl} is the totally antisymmetric tensor ($i, j, k, l = 1, \ldots, 4$) and the term proportional to F is not allowed for $N \neq 4$. The spectrum of Eq. (73) and the degeneracy of each level are listed in the top part of Table IV.

Since the group SO(4) is isomorphic to SU(2) $\otimes$ SU(2), an equivalent way of thinking about the SO(4) Hamiltonian is in terms of two spins-1/2 per site. Let us make the connection between the two languages. Denoting the two spin-1/2 degrees of freedom by $\mathbf{S}$ and $\mathbf{T}$, the most general two-site SU(2) $\otimes$ SU(2)-invariant Hamiltonian has the following form:

$$\mathcal{H}_{KK} = B_0 + B_1\mathbf{S}_1 \cdot \mathbf{S}_2 + B_2\mathbf{T}_1 \cdot \mathbf{T}_2 + B_{12}(\mathbf{S}_1 \cdot \mathbf{S}_2)(\mathbf{T}_1 \cdot \mathbf{T}_2). \quad (74)$$

This is the well-known Kugel-Khomskii model [26]. Two of its good quantum numbers are associated with $\mathbf{T}_T^2 = (\mathbf{T}_1 + \mathbf{T}_2)^2$ and $\mathbf{S}_T^2 = (\mathbf{S}_1 + \mathbf{S}_2)^2$ and can be used to label the eigenstates of the Hamiltonian. The energy levels and the corresponding quantum numbers associated with $\mathbf{T}_T^2 = T_T(T_T + 1)$ and $\mathbf{S}_T^2 = S_T(S_T + 1)$ are represented on the right-hand side of Table IV. The equivalence between Eqs. (73) and (74) is obtained with the following relations:

$$B_0 = \frac{3}{2}D, \quad (75)$$

$$B_1 = 2(J - D - 4F), \quad (76)$$

$$B_2 = 2(J - D + 4F), \quad (77)$$
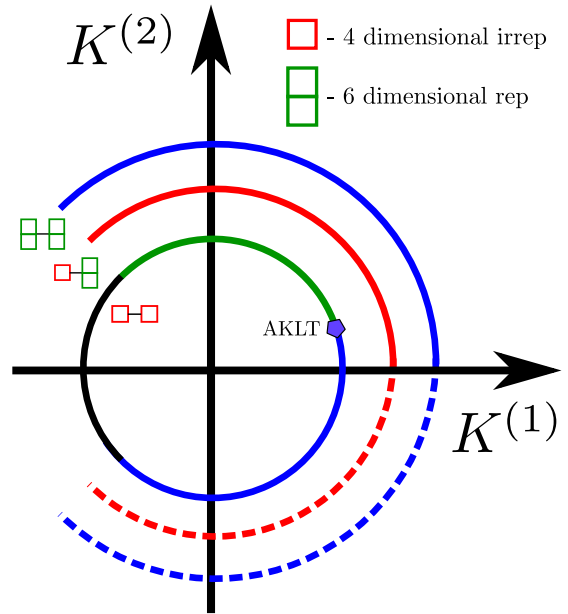
$$B_{12} = 8D. \quad (78)$$

FIG. 8. Ground-state structure of the SO(4) two-site problem as a function of the angle θ, with different colors representing the distinct multiplets. Dashed lines correspond to different representations of the same dimension as their corresponding color. The singlet state is represented in blue while the fundamental representation [1, 0] (single box, in Young-tableau notation) in shown in red and the 6-dimensional representation [1, 1] (two boxes) in green (cf. Fig. 4). Unlike in the odd-N case, the two-site gap closes at $\theta = 0$, which makes the RG flow ill defined, except when the fundamental representation of the group is realized on both sites (inner circle).

In order to make the SO(4)-symmetric Hamiltonian similar to the other SO(2N) models, we will set $F = 0$ in Eq. (73). The case where F is nonzero leads to an SDRG flow which cannot be treated with the approach described in this paper. Setting $F = 0$ is equivalent to setting $B_1 = B_2$ in (74). In this case, there is an additional $\mathbb{Z}_2$ symmetry related to the exchange $\mathbf{S} \rightleftarrows \mathbf{T}$. With this choice, the two triplet representations of SO(4) become degenerate (see Table IV), and the RG structure becomes identical to any other SO(2N) model.

In general, the RG flow for SO(4) is almost identical to the case we described for odd N, with one remarkable difference: the low-energy physics of the region between the AKLT point $\theta_0 = \arctan\frac{1}{3}$ and $\theta_0 = \frac{\pi}{4}$ is ill controlled within the SDRG framework we are describing here. In that region, the initial RG structure is very similar to the case described for odd N. The representation [1, 1] is generated and SDRG rules that include such representation are also necessary. As the SDRG proceeds, the angle distribution starts flowing to a delta function at $\theta = 0$. The two outermost circles of Fig. 8 show that the local two-site gap closes at $\theta = 0$ when a pair of sites with representations [1, 1]-[1, 0] or [1, 1]-[1, 1] are coupled. Since a large local gap is required for the validity of perturbation theory, this makes the SDRG flow ill defined asymptotically. In order to probe the physics of this region one has to go beyond the current SDRG framework, keeping more than one multiplet when a pair of sites is decimated, in a similar fashion to what was done in Refs. [14,15] in a different context. Again, this falls outside the scope of this work.
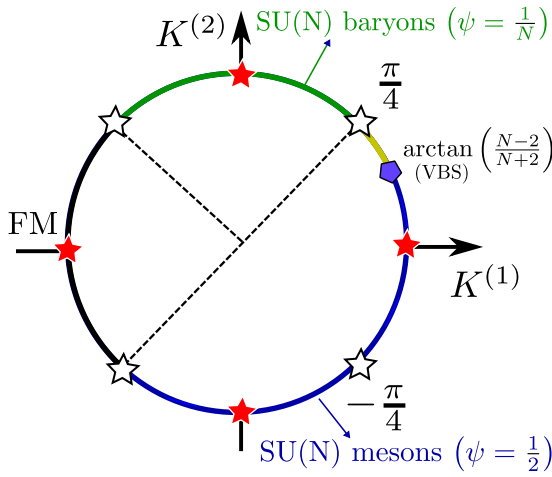
FIG. 9. The SO(N) spin chain phase diagram, reproduced from Ref. [27]. Red stars correspond to stable SDRG fixed points, while white ones correspond to the unstable fixed points. The point $\pi/4$ is SU(N) symmetric, with the spins in the fundamental representation of the group. The point $-\pi/4$ is also SU(N) symmetric, with the fundamental and antifundamental representations on alternating sites. The black arc denotes the ferromagnetic region, beyond the scope of this work. The points $\pm 3\pi/4$ fix the transition between the baryonic and mesonic phases to the ferromagnetic region. The region between the AKLT point ($\tan\theta = \frac{N-2}{N+2}$) and the SU($N$)-symmetric point $\pi/4$ results either in an uncontrolled SDRG flow, for even N, or in a basin of attraction equivalent to the blue region, for odd N.

Outside this problematic region, the SDRG flow has the same structure as the odd-N case of the previous section. There is a mesonic phase for $-3\pi/4 < \theta_0 < \arctan\frac{1}{3}$ with two possible angular fixed points and $\psi_M = 1/2$. If $-3\pi/4 < \theta_0 < -\pi/4$, the flow is toward $\theta = -\pi/2$, whereas the angular fixed point is $\theta = 0$ if $-\pi/4 < \theta_0 < \arctan\frac{1}{3}$. For $\pi/4 < \theta_0 < 3\pi/4$, the phase is baryonic (with singlets made out of $4k$ original spins), the angular fixed point is $\theta = \pi/2$, and $\psi_B = 1/4$.

The SDRG flow and phase diagram for larger, even values of N are identical to those described for SO(4) although more representations are generated, as shown in Fig. 9. The region $\arctan(\frac{N-2}{N+2}) < \theta_0 < \frac{\pi}{4}$ suffers the same problems as in SO(4) and cannot be properly treated with the current SDRG scheme (yellow region of Fig. 9). The mesonic and baryonic phases are shown as blue and green in Fig. 9, respectively. The former is characterized by $\psi_M = 1/2$ whereas the latter has $\psi_B = 1/N$. If we conventionalize that for odd N, the yellow region has the same physics as the blue one, Fig. 9 encapsulates the phase diagram of all SO(N)-symmetric disordered spin chains.

C. The Sp(N) group

We now address Sp(N)-symmetric models. As Sp(N) is a subgroup of SU(N), by fine-tuning the angle parameter the symmetry can be explicitly enhanced, just as in the SO(N) case [see Eq. (20)]. The SU(N)-symmetric points are again at $\pm\frac{\pi}{4}$ and $\pm\frac{3\pi}{4}$. There is, however, a remarkable difference between these high-symmetry points, when compared to the SO(N) case. In SO(N) chains, the level structure at the angle
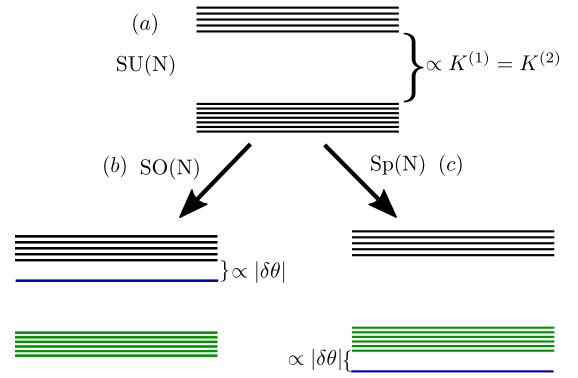

FIG. 10. Schematic energy levels close to the point $\frac{\pi}{4}$, in terms of the angular deviation $\delta\theta = |\theta - \frac{\pi}{4}| \ll 1$. (a) At the point $\frac{\pi}{4}$, the Hamiltonian has explicit SU(N) symmetry, and the degeneracies are $\frac{N(N-1)}{2}$ (ground multiplet) and $\frac{N(N+1)}{2}$ (excited multiplet). (b) Adding a small perturbation that breaks the SU(N) symmetry into SO(N), the excited multiplet splits into levels with an $\frac{N(N+1)}{2} - 1$ degeneracy and a singlet, while the low-energy multiplet remains the same. (c) Now, slightly breaking SU(N) into Sp(N). The lowest-energy state is a singlet (blue), separated from the first excited multiplet by a small gap proportional to $|\delta\theta|$.

$\frac{\pi}{4}$ is such that two *excited states* of the two-site problem have the same energy. In Sp(N) systems, on the other hand, the *two lowest-lying multiplets* become degenerate at the angle $\frac{\pi}{4}$. This can be predicted by directly looking at the degeneracies of the Sp(N) multiplets, and comparing them to the SU(N) degeneracies. The breaking of SU(N) into SO(N) or Sp(N) in terms of energy levels of a two-site problem is shown in Fig. 10. In contrast with SO(N), where the decimations are well defined around this high-symmetry point, in Sp(N) the local two-spin gap is proportional to $\delta\theta = |\theta - \frac{\pi}{4}|$. If $\delta\theta$ is small, the SDRG as proposed in this work cannot be applied.

Still, there are regions of the phase diagram that can be safely analyzed with our method. In order to characterize the AF phases, we again assume that the initial angle is fixed. If the initial angle is $\arctan(\frac{N+2}{N-2}) < \theta_0 < \frac{\pi}{4}$ (blue region of Fig. 11), and as long as θ_0 is far enough from the $\frac{\pi}{4}$ point such that the SDRG is consistent, the distribution of angles will broaden at early RG stages. After some transient, however, the distribution converges to a delta function at either 0 or $-\frac{\pi}{2}$, which are the only stable angular fixed points in this region (see Fig. 10), characterized by $\psi_M = 1/2$. Again, just like in the SO(N) case, the point $-\frac{\pi}{4}$ has a higher SU(N) symmetry and corresponds to an unstable angular fixed point. The basins of attraction of $\theta = 0$ and $\theta = -\frac{\pi}{2}$ are $-\frac{\pi}{4} < \theta_0 < \frac{\pi}{4}$ and $\arctan(\frac{N+2}{N-2}) < \theta_0 < -\frac{\pi}{4}$, respectively.

The most striking difference between SO(N) and Sp(N) chains appears when the initial angle is in the range $\frac{\pi}{4} < \theta_0 < \frac{3\pi}{4}$ (dashed line of Fig. 11). First, since there is no SU(N)-symmetric point inside this region, the shortcut we used to derive the prefactors of the SDRG equations cannot be used. The generic rules for first-order decimations [Eq. (31)] are still valid, but, in order to determine the prefactors, the Sp(N) tensors have to be constructed explicitly on a case-by-case basis. Determining these factors is mandatory to follow the SDRG flow, particularly since under certain conditions, our
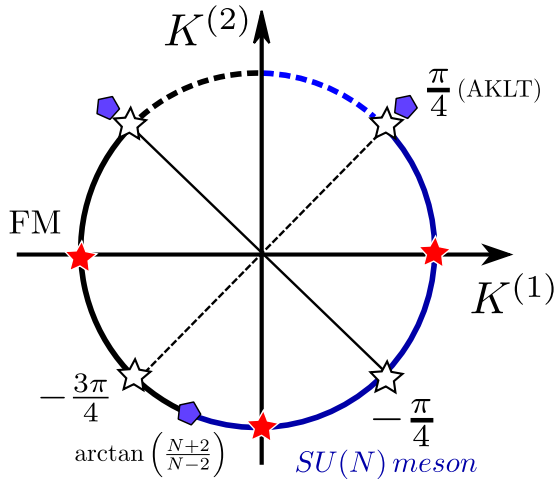
FIG. 11. The phase diagram of Sp(N)-symmetric chains, with $N = 4, 6$. For $\arctan \frac{N+2}{N-2} < \theta < \frac{\pi}{2}$, the system is in a mesonic SU(N) random singlet phase. Otherwise, it is in a ferromagnetic-like phase. The pentagons represent the angles where two multiplets cross as ground states. The white stars correspond to unstable angular fixed points, while the red ones are the stable angular fixed points. Notice that there is no baryonic phase in Sp(N). Colors match their corresponding basins of attraction; the flow of the dashed lines is described in the main text.

first-order RG rules become ill defined when the proportionality constants vanish (see Sec. IV A). To see this concretely, let us consider the cases of Sp(4) and Sp(6) as examples, and discuss the general features that are expected to appear for larger N. For Sp(4) the coupling $K^{(2)}$ is renormalized to zero due to the structure of the Clebsch-Gordan series [case (i) of Sec. IV A]. For $\frac{\pi}{4} < \theta_0 < \frac{3\pi}{4}$, the following Clebsch-Gordan series are relevant [34]:

$$
\begin{aligned}
4 \otimes 4 &= 1 \oplus 5 \oplus 10, \\
4 \otimes 5 &= 4 \oplus 16, \\
5 \otimes 5 &= 1 \oplus 10 \oplus 14, \\
5 \otimes 10 &= 5 \oplus 10 \oplus 35,
\end{aligned}
\tag{79}
$$

where we labeled the representations by their dimensions. Recall that for a pair of representations Υ and Υ', $P_\Upsilon T^{\Upsilon'} P_\Upsilon \neq 0$, P_Υ being a projection operator onto representation Υ, only if Υ' belongs to the Clebsch-Gordan series of $\Upsilon \otimes \Upsilon$. Starting with the fundamental representation of dimension 4 on each site, initial RG steps generate the 5-dimensional representations via first-order decimations. After some steps, unavoidably, a decimation of a 5-dimensional representation coupled to a 4-dimensional representation happens. Let us label the Sp(4) tensors by T^{10} (coupled by $K^{(1)}$) and T^5 (coupled by $K^{(2)}$), using the shorthand notation of labeling the representations by their dimension. Now, since

$$
\begin{aligned}
P_5 T^{10} P_5 &\neq 0, \\
P_5 T^5 P_5 &= 0,
\end{aligned}
\tag{80}
$$

the renormalized $K^{(2)}$, which is proportional to $P_5 T^5 P_5$, is zero. A similar renormalization to zero has been found in SU(2)-symmetric spin-S chains with $S > 1$ [17]. As a consequence, the low-energy physics is dominated by $K^{(1)}$ only. The initial sign of $K^{(1)}$ thus becomes crucial, and a distinction has to be made depending on whether θ_0 is greater or smaller than $\frac{\pi}{2}$. If $\frac{\pi}{2} < \theta_0 < \frac{3\pi}{4}$, the renormalization projects $(K^{(1)}, K^{(2)})$ into the $K^{(1)} < 0$ semiaxes, and the phase is ferromagnetic and thus outside the scope of our analysis. If, on the other hand, the initial angle lies in the interval $\frac{\pi}{4} < \theta_0 < \frac{\pi}{2}$, the projection makes the flow identical to the one starting with $\theta = 0$, and the low-energy physics is again an RSP with $\psi_M = \frac{1}{2}$.

Similar reasoning can be applied to Sp(6). Here the important Clebsch-Gordan series read [34]

$$
\begin{aligned}
6 \otimes 6 &= 1 \oplus 14 \oplus 21, \\
14 \otimes 6 &= 6 \oplus 14' \oplus 64, \\
14' \otimes 6 &= 14 \oplus 70, \\
14 \otimes 14' &= 6 \oplus 64 \oplus 126, \\
14 \otimes 14 &= 1 \oplus 14 \oplus 21 \oplus 70 \oplus 90, \\
14' \otimes 14' &= 1 \oplus 21 \oplus 84 \oplus 90, \\
14' \otimes 21 &= 14' \oplus 64 \oplus 216.
\end{aligned}
\tag{81}
$$

Notice that the representations $14'$ and 14 are different, even though they have the same dimension. The tensors of interest are T^{14} (coupled by $K^{(1)}$) and T^{21} (coupled by $K^{(2)}$). In the region of interest, initial RG steps generate representations of dimension 14, which, when coupled to the fundamental representation, enforces $14'$ as the ground state. From the Clebsch-Gordan series above, $P_{14'} T^{14} P_{14'} = 0$, while $P_{14'} T^{21} P_{14'} \neq 0$.

We have checked that for Sp(8) and Sp(10) these renormalizations to zero do not appear, which means that these features are most likely a property present for low N only. A different issue arises, however, by a similar analysis of the Clesbch-Gordan series [34], we find that a large number of representations are generated in early RG steps, as opposed to the SO(N) flow, where the number of representations appearing when $\frac{\pi}{4} < \theta_0 < \frac{3\pi}{4}$ is always int($N/2$). At this stage, the Sp(N) problem might lead then to either a ferromagnetic phase, or a so-called large spin phase (LSP) [38], also common in disordered spin chains. Another possibility is that these large representations disappear at low energies. The only way to see which one actually happens is to construct the tensors from their definition [Eq. (9)] for all these representations, as well as the prefactor of the RG rules [Eqs. (31) and (41)], a very challenging task. Physically, since the most relevant Sp(N) cases are the ones with small N, we will not pursue a further analysis here.

VI. EMERGENT SU(N) SYMMETRY

In the previous sections, we characterized the SDRG flow by determining the AF phases as well as their exponent ψ. A more subtle feature of the RSPs displayed above is the emergence of SU(N) symmetries. In this section, we show the mechanism responsible for the symmetry enhancement. An overall explanation has been given in Ref. [27], and here we complement it with further details.

We would like to emphasize the generality of this result. Notice that we have studied all the random antiferromagnetic spin chain models invariant under transformations of

the semisimple Lie groups, Sp(N), SO(N), and, consequently, the SU(N). We have focused, however, only on the case in which the spins are represented only by totally antisymmetric representations of the group.

Let us start with the SO(N) case. The scalar operators that constitute Hamiltonian (17) are formed out of tensor operators $T_v^{[1,1]}$ and $T_v^{[2,0]}$. These operators have a physical interpretation similar to the vector and quadrupolar operators in SU(2) [20], and their response functions are not expected to be generically the same. Indeed, thinking of the SO(N) problem as an anisotropic SU(N) model, the uniform susceptibilities associated with the SU(N) generators are

$$\chi_\mu = \beta\big(\langle \Lambda_T^\mu \rangle^2 - \langle (\Lambda_T^\mu)^2 \rangle\big). \tag{82}$$

If the Hamiltonian of the problem displays an SO(N)-preserving SU(N) anisotropy, no reason *a priori* exists to expect the responses involving the Λ^μ chosen from any of the $N(N-1)/2$ SU(N) purely imaginary generators [$\sim T_v^{[1,1]}$ in SO(N)] to be the equal to those of the remaining $N(N+1)/2 - 1$ SU(N) purely real ones [$\sim T_v^{[2,0]}$ in SO(N)]. Yet, as we explain below, in the RSPs the singular behavior is isotropic and equal to that of an SU(N)-invariant system.

Our argument is supported by two key observations: (i) each SO(N) representation that appears throughout the SDRG flow has an SU(N) counterpart and (ii) the 2-site ground states at the stable angular fixed points $0, -\pi/2$ $(+\pi/2)$ are identical to those of the SU(N)-symmetric points $-\pi/4$ $(+\pi/4)$. The direct consequence of points (i) and (ii) is that if the angular distribution starts at the stable fixed points, the SDRG flow at low energies is indistinguishable from the flow started at the SU(N)-symmetric points, for the following reasons. Point (i) guarantees that the representations generated in the flows within the mesonic and baryonic phases always find counterparts in the SU(N) representation spectrum, so any remaining nondecimated spin at low energies still defines an object transforming in the full SU(N) group. Furthermore, through point (ii), the local two-spin gaps never close for angles between 0 and $-\pi/2$, which includes the SU(N)-symmetric mesonic point $-\pi/4$, or between the SU(N)-invariant baryonic point $\pi/4$ and $\pi/2$. Adding to this the fact that the unstable SU(N)-symmetric points are contained in the corresponding mesonic/baryonic AF basins of attraction, one finally realizes that all the two-site ground multiplets generated throughout the flow are SU(N) invariant. In sum, points (i) and (ii) guarantee that both the ground state and the collection of free spins at finite low energies are composed of SU(N)-invariant objects. A difference between the flows at the SU(N)-symmetric points and those of the stable angular fixed points does remain. It lies in the fact that the decimation rules for the radii r_i have distinct prefactors depending on the bond angle. Since the radial disorder grows without bounds in RSPs, however, the prefactors are asymptotically irrelevant.

Combining the points above, we conclude that the ground state of the system is an SU(N)-invariant state composed of a collection of SU(N) singlets, while the low-energy physics of the chain is governed by free spins in SU(N) antisymmetric representations. From this, thermodynamic quantities,

such as the magnetic susceptibilities, follow immediately. The calculation of the magnetic susceptibility χ_μ for a single free spin Λ^μ gives Curie's law $\chi_\mu^{\text{free}} \sim T^{-1}$, independently of μ. The total susceptibility is then obtained by multiplying by the density of free spins at energy scale $\Omega = T$, $\chi_\mu(T)^{-1} \sim T L_T \sim T |\ln T|^{1/\psi}$, which is controlled by the universal exponent ψ [27]. The impact of the distinct prefactors of the SDRG decimation equations is only in the nonuniversal behavior of the prefactors, but not in the universal exponents.

Both RSPs are then composed of collections of completely frozen pairs or kN-tuples of spins and low-energy free spin excitations which actually transform as irreducible representations of SU(N). As discussed in Sec. V we make an analogy with quantum chromodynamics and we call the two AF phases mesonic or baryonic. If the ground state is a collection of two-site singlets, we have the *mesonic RSP,* with tunneling exponent $\psi_M = 1/2$. For $N = 2$, this is just the standard RSP phase for XXZ spin-1/2 chains, which are SU(2) anisotropic but which indeed display emergent SU(2) symmetry at low energies [3,5]. If, on the other hand, the phase is characterized by a collection of singlets formed out of multiples of N spins, then we have the *baryonic RSP.* This phase has a tunneling exponent $\psi_B = 1/N$. Crucially, these tunneling exponents are indeed the same ones found previously by two of us in the context of SU(N)-symmetric disordered spin chains [35].

While the baryonic RSP is generically attainable for SO(N) Hamiltonians, we see that it is not in the Sp(N) case, which displays only mesonic phases (due to the adiabaticity argument for $\theta = -\pi/4$; see Fig. 11). This a striking distinction arising from the fact that the other SU(N)-symmetric point, $\theta = +\pi/4$, is located now at a ground multiplet degeneracy point (AKLT) (again, see Fig. 11). At that point, our SDRG rules break down and a more refined analysis must be made on a case-by-case basis.

Finally, another hallmark of the emergent symmetry phenomenon is the ground-state spin-spin correlation function $C_{i,j}^\mu = \langle \Lambda_i^\mu \Lambda_j^\mu \rangle$ (μ label not summed). As we have just shown, the ground state of the anisotropic model is identical to the isotropic one in the RSP within the approximation of the SDRG method. Since the singular behavior is captured exactly (asymptotically) by the SDRG method, it is then a straightforward conclusion that in the RSPs here reported $C_{i,j}^\mu = C_{i,j}$ as far as the singular behavior is concerned. Therefore, the mean $\overline{C_{i,j}^\mu}$ and typical $C_{i,j}^{\mu,\text{typ}}$ values of the correlation function are those of the SU(N)-symmetric models, already reported in the literature [35,41]. Thus,

$$\overline{C_{i,j}^\mu} \sim |i - j|^{-\eta_\mu}, \tag{83}$$

with universal exponent $\eta_\mu = \eta = 2$ (both in the mesonic and baryonic phases), and

$$C_{i,j}^{\mu,\text{typ}} \sim \exp - \left| \frac{i-j}{\xi} \right|^\psi, \tag{84}$$

with the universal tunneling exponent ψ (which is either $\psi_M = \frac{1}{2}$ or $\psi_B = \frac{1}{N}$). Here ξ is a nonuniversal length scale

on the order of the crossover length between the clean and the infinite-randomness fixed points.

VII. RSP SIGNATURES IN HIGHER-ORDER SUSCEPTIBILITIES

A naturally relevant question regards how to detect signatures of symmetry emergence. In Sec. VI, we mentioned that such signatures can be seen in the linear susceptibilities of $T_v^{[1,1]}$ and $T_v^{[2,0]}$ operators. These tensors present the same low-temperature dependence, even though this is not obvious *a priori*, given the anisotropy of the underlying Hamiltonian. Since the possible realizations of SO(N) chains have very different microscopic origins, it is difficult to give a generic prescription of how to access such susceptibilities, i.e., one that is valid for any value of N.

To make progress, we attempt to draw inspiration from a concrete case: $N = 3$ (the spin-1 chain). In this case, the $T_v^{[1,1]}$ operators are the usual spin-1 (vector) operators S_x, S_y, and S_z and their corresponding linear susceptibilities are the usual magnetic susceptibilities. The $T_v^{[2,0]}$ operators are the spin-1 quadrupolar operators $(3S_z^2 - 2)/\sqrt{3}$, $S_x^2 - S_y^2$, $S_x S_y + S_y S_x$, $S_x S_z + S_z S_x$, and $S_y S_z + S_z S_y$ [20]. Since these $T_v^{[2,0]}$ operators involve products of the vector operators, it is suggestive that higher-order, *nonlinear* susceptibilities of $T_v^{[1,1]}$ might serve as a window to study *linear* susceptibilities of $T_v^{[2,0]}$, thus serving as a good route to distinguish RSPs with and without symmetry enhancement. For example, for $N = 3$, inspection of the first quadrupolar operator ($\sim S_z^2 + \text{const}$) naively suggests that the first nonlinear magnetic susceptibilities might come in handy.

So we take here a position: in the general scenario, we assume that $T_v^{[1,1]}$ susceptibilities are easier to access and ask whether we could use nonlinear susceptibilities of $T_v^{[1,1]}$ to probe $T_v^{[2,0]}$ and, therefore, the symmetry enhancement. We show, however, that the structure of the RSPs is such that this is, in fact, incorrect. Nonlinear responses of $T_v^{[1,1]}$ operators show no distinction between phases with and without symmetry enhancement.

Let us denote by $\Lambda^\mu = \sum_{i=1}^{N_s} \Lambda_i^\mu$ the total value (summed over all N_s sites) of the μth SU(N) generator ($\mu = 1, \ldots, N^2 - 1$). As explained before, the first $N(N + 1)/2$ of these are the generators of SO(N) (the $T_v^{[1,1]}$ operators), whereas the remainder [$\mu = N(N + 1)/2 + 1, \ldots, N^2 - 1$] are the $T_v^{[2,0]}$ tensor operators of SO(N). Coupling external fields to these quantities $H \rightarrow H + h_\mu \Lambda^\mu$, the expressions for the linear and the first nonzero nonlinear susceptibilities can be obtained as

$$\chi_\mu^{(1)} = \left. \frac{\partial \langle \Lambda^\mu \rangle}{\partial h_\mu} \right|_{h_\mu \to 0} = \frac{1}{T} [\langle (\Lambda^\mu)^2 \rangle - \langle \Lambda^\mu \rangle^2], \quad (85)$$

$$\chi_\mu^{(3)} = \left. \frac{\partial^3 \langle \Lambda^\mu \rangle}{\partial h_\mu^3} \right|_{h_\mu \to 0} = \frac{1}{T^3} [\langle (\Lambda^\mu)^4 \rangle - 4 \langle \Lambda^\mu \rangle \langle (\Lambda^\mu)^3 \rangle$$
$$- 3 \langle (\Lambda^\mu)^2 \rangle^2 + 12 \langle \Lambda^\mu \rangle^2 \langle (\Lambda^\mu)^2 \rangle - 6 \langle \Lambda^\mu \rangle^4], \quad (86)$$

where $\langle \mathcal{O} \rangle$ represents the thermal expectation value of $\mathcal{O}$. In the absence of symmetry breaking $\langle \Lambda^\mu \rangle = 0$ and the

expressions simplify to

$$T \chi_\mu^{(1)} = \langle (\Lambda^\mu)^2 \rangle, \quad (87)$$

$$T^3 \chi_\mu^{(3)} = \langle (\Lambda^\mu)^4 \rangle - 3 \langle (\Lambda^\mu)^2 \rangle^2$$
$$= \langle (\Lambda^\mu)^4 \rangle - 3T^2 [\chi_\mu^{(1)}]^2. \quad (88)$$

We want to write SDRG results for these quantities in the limit $h_\alpha \ll T$ in the various random singlet phases. Stopping the SDRG flow when the largest coupling Ω reaches some low temperature T, there are asymptotically two types of objects left: free spins, with density $n(T) \sim 1/L_T \sim |\ln T|^{-1/\psi}$, and strongly bound SO($N$) singlets, with density $\propto 1 - n(T)$. The actual density of singlets depends on how many original spins are required to form them. In the mesonic phases, this is $[1 - n(T)]/2$. In the baryonic ones, in which singlets are composed of kN original spins, it is $[1 - n(T)]/\bar{k}N$, where $\bar{k} \gtrsim 1$ is the average value of k. In general, the linear susceptibilities can then be written as

$$T \chi_\mu^{(1)} \sim n(T) \langle (\Lambda_{i_0}^\mu)^2 \rangle_{\text{free}} + \frac{1 - n(T)}{C} \langle (\Lambda^\mu)^2 \rangle_{\text{singlet}}, \quad (89)$$

where $C = 2$ or $\bar{k}N$, whichever is the case, and the expectation values should be calculated in the ground multiplets, either a free spin or a random singlet. In this equation, i_0 labels an arbitrary free spin site and $\Lambda^\mu = \sum_{i=1}^{kN} \Lambda_i^\mu$, where the sum is over all the kN spins within a singlet. The expectation values of the free spins are independent of i_0. Analogously,

$$T^3 \chi_\mu^{(3)} + 3T^2 [\chi_\mu^{(1)}]^2 \sim n(T) \langle (\Lambda_{i_0}^\mu)^4 \rangle_{\text{free}}$$
$$+ \frac{1 - n(T)}{C} \langle (\Lambda^\mu)^4 \rangle_{\text{singlet}}. \quad (90)$$

Let us now analyze separately the cases of SO(N) $T_v^{[1,1]}$ and $T_v^{[2,0]}$ operators. For the sake of clarity, we will use labels $\mu \rightarrow \alpha \in [1, \ldots, N^2 - 1]$ for the former and $\mu \rightarrow \beta \in [N(N + 1)/2 + 1, \ldots, N^2 - 1]$ for the latter. Now, since the SO(N) singlets are annihilated by the total SO(N) generators, $\langle (\Lambda^\alpha)^2 \rangle_{\text{singlet}} = \langle (\Lambda^\alpha)^4 \rangle_{\text{singlet}} = 0$. Thus, for the $T_v^{[1,1]}$ operators,

$$T \chi_\alpha^{(1)} \sim n(T) \langle (\Lambda_{i_0}^\alpha)^2 \rangle_{\text{free}} \quad (91)$$

and

$$T^3 \chi_\alpha^{(3)} + 3T^2 [\chi_\alpha^{(1)}]^2 \sim n(T) \langle (\Lambda_{i_0}^\alpha)^4 \rangle_{\text{free}}. \quad (92)$$

This equation is the main finding of this section. Equation (92) is completely expressed in terms of SO(N) labels α and is, in general, unrelated to $\chi_\beta^{(1)}$. This expression is the same for arbitrary RSPs independently of symmetry emergence (see especially the following section, Sec. VIII). In summary, nonlinear susceptibilities are not useful in assessing whether or not an RSP displays symmetry emergence.

The result above is in strong contrast to the linear susceptibility of tensor SO(N) operators $\chi_\beta^{(1)}$, which is, indeed, a probe of symmetry enhancement as shown before. Let us briefly revisit the argument for completeness. If the SO(N) singlet is also an SU(N) singlet, a necessary ingredient for the emergent symmetry, then the linear susceptibilities for tensors

$T_v^{[2,0]}$ also obey

$$\langle (\Lambda^\beta)^2 \rangle_{\text{singlet}} \underbrace{=}_{\text{ES}} 0, \tag{93}$$

where "ES" indicates the presence of an emergent symmetry. This is the case since the Λ^β are also SU(N) generators and, therefore, annihilate SU(N) singlets. In summary, neglecting nonuniversal prefactors,

$$\chi_\beta^{(1)} \sim \begin{cases} \frac{n(T)}{T} \langle (\Lambda_{i_0}^\beta)^2 \rangle_{\text{free}} \sim \frac{1}{T|\ln T|^{1/\psi}}, & \text{if ES}, \\ \frac{1-n(T)}{CT} \langle (\Lambda_{i_0}^\beta)^2 \rangle_{\text{singlet}} \sim \frac{1}{T}, & \text{otherwise}, \end{cases} \tag{94}$$

indeed distinct from what we see for $\chi_\alpha^{(1)}$ in Eq. (92), which is always true and $\sim n(T)/T$.

VIII. AN RSP WITHOUT EMERGENT SYMMETRY

So far we have focused on a fairly general class of models with manifest SO(N) symmetry in which RSPs displaying a larger SU(N) symmetry emerge at low energies. The question then arises: is there a counterexample to this situation, namely, a model with an RSP phase in which no larger symmetry emerges? What physical consequences would follow in that case? We will now show a specific model in which this does indeed happen.

Consider a dimerized SO(4) chain governed by the Hamiltonian of Eq. (17) with $K_i^{(1)} = 0$ for every i (this restriction can be relaxed but it makes the argument more transparent). The values of the $K_i^{(2)}$ couplings are random and depend on whether they are on odd, $K_{i,o}^{(2)} \equiv K_{2i+1}^{(2)}$, or even, $K_{i,e}^{(2)} \equiv K_{2i}^{(2)}$, bonds. The odd couplings are taken to be strictly positive and much larger than the absolute values of the couplings on even bonds $K_{i,o}^{(2)} \gg |K_{i,e}^{(2)}|$. The even couplings can be either all positive or all negative. This is shown schematically in Figs. 12(a) and 12(b), respectively.

We now refer to the ground multiplet structure of a pair of spins, as shown in Fig. 8. In the initial stages of the RG, only odd bonds will be decimated and this will give rise to effective spins transforming as the 6-dimensional representation of SO(4); see the innermost arc of Fig. 8. Since these decimations are performed in first order of perturbation theory, the distribution of even bonds will not change appreciably. Moreover, the signs of the even bonds will remain the same: either all positive or all negative, as given by Eq. (48) with $\xi_{1,3} = 1$ and $\Phi_{1,3} = 1/2$. After all the odd bonds have been decimated, we will be left with an effective chain of spins belonging to the 6-dimensional representation of SO(4) with random $K_{i,e}^{(2)}$ couplings only, either all positive or all negative. This is shown schematically in Fig. 12(c).

The next decimations will be governed by the outermost arc of Fig. 8. At each decimation, the ground state is always a singlet. From Eq. (61), the decimation rule, particularized to the case of $N = 4$ and $Q = 2$ (the 6-dimensional representation), is

$$\tilde{K}_{1,4,e}^{(2)} = \frac{1}{3} \frac{K_{1,e}^{(2)} K_{3,e}^{(2)}}{K_{2,e}^{(2)}}. \tag{95}$$

Recall that here, sites 2 and 3 are removed from the chain and an effective coupling between sites 1 and 4 is generated.
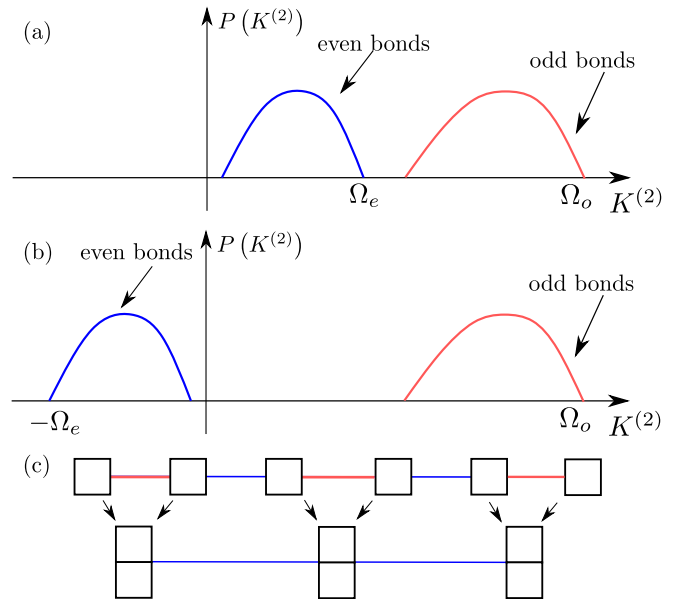

FIG. 12. An SO(4)-symmetric chain without an emergent SU(4) symmetry. (a) and (b) Initial probability distributions of even (blue) and odd (red) bonds. In (a), the even bonds have $K_{i,e}^{(2)} > 0$, which corresponds to the case with an emergent SU(4) symmetry. In (b), $K_{i,e}^{(2)} < 0$, the case where there is no symmetry enhancement. (c) Evolution of the nondecimated sites as the RG scale Ω runs in the range $\Omega_e \lesssim \Omega \lesssim \Omega_o$. The odd-bond distribution has a cutoff $\Omega_o \gg \Omega_e$ such that these bonds will all be decimated first, generating 6-dimensional representations connected by blue bonds.

Note also that the decimation rule is valid for any sign of the couplings and thus preserves the signs of the initial distribution.

Even though the ground state is always a singlet, two possible kinds of singlets can be formed, depending on the sign of $K_{i,e}^{(2)}$. Remarkably, only the singlet formed when $K_{i,e}^{(2)} > 0$ is also an SU(4) singlet (the continuous blue line of the the the outermost arc of Fig. 8). When $K_{i,e}^{(2)} < 0$, by contrast, the singlet is not an SU(4) singlet (the dashed blue line of the outermost arc of Fig. 8). As a result, while the former situation exhibits an emergent SU(4) symmetry, as described in the previous section, Sec. VII, the latter one does not. This will be clearly reflected in the physical properties as we will now show.

The crucial impact of having $K_{i,e}^{(2)} < 0$ is that the contributions from the singlets no longer vanish in the linear susceptibilities of the tensor operators; see Eq. (89). Physically, an external field coupled to the tensor operators is able to polarize the singlets, as opposed to the effect of a field coupled to the SO(N) generators. Explicitly, if the singlets are formed by coupling the 6-dimensional spins at sites i and $i + 1$, the expectation value of tensor operators can be calculated for SO(4) to be

$$\langle (\Lambda_i^\beta + \Lambda_{i+1}^\beta)^2 \rangle_{\text{singlet}} = \frac{8}{3}. \tag{96}$$

Thus, using $n(T) \ll 1$, (89) now gives the leading low-temperature behavior

$$\chi_\beta^{(1)} \sim \frac{1}{T}. \tag{97}$$

Even though the singlets in this case are not SU(4) singlets they are obviously still SO(4) singlets. Therefore, their contributions to the nonlinear susceptibilities of the generators remain zero, and Eq. (92) is still valid:

$$T^3 \chi_\alpha^{(3)} + 3T^2 \big[\chi_\alpha^{(1)} \big]^2 \sim \frac{1}{|\ln T|^{1/\psi}} \underset{\text{no ES}}{\neq} T \chi_\beta^{(1)}, \qquad (98)$$

where "no ES" means that we are dealing with a situation in which there is no emergent symmetry. We thus see that the connection between the nonlinear susceptibilities of vector operators and the linear susceptibilities of tensor ones cannot be established in this case. Other counterexamples can be constructed for other even values of N.

IX. DISCUSSION AND CONCLUSIONS

A. General results

We have determined the ground-state structure and the low-temperature thermodynamic properties of disordered spin chains invariant under transformations of a large class of Lie groups [SO(N), Sp(N)] in the strong-disorder limit. We have determined the phase diagram and fully characterized the phases when the spins belong to the totally antisymmetric representations of the groups (which include the fundamental one). When the chains have special orthogonal SO(N) or symplectic Sp(N) symmetries at the microscopic level, these phases share the same physics of chains which are symmetric under transformations of the larger special unitary SU(N) group, even though the microscopic fixed-point Hamiltonian does not have such enlarged symmetry. This is the defining characteristic of a system exhibiting symmetry emergence, exposed here by the way the ground state and low-energy excitations transform under SU(N) rotations.

Two distinct phases are found; both of them are critical and governed by infinite-randomness fixed points. The transition between them is also governed by an infinite-randomness fixed point, albeit with exact SU(N) symmetry. Thus, our methods are asymptotically exact in their fixed-point basins of attraction. The ground states in both phases and at the transition point are composed of SU(N) singlets and thus these phases are of the random-singlet type. The distinction between these phases stems from the structure of the singlets. In the meson-like phase, the singlets are composed by only two spins whereas in the baryon-like phase [which occurs only for the SO($N > 2$) cases], the singlets are composed by multiples of N spins.

As shown in Sec. VI, two critical and disorder-independent exponents describe the asymptotic behavior of these critical phases: the tunneling exponent ψ ($\psi_M = \frac{1}{2}$ and $\psi_B = \frac{1}{N}$ in the mesonic and baryonic phases, respectively), which governs the low-temperature thermodynamics, the typical value of the ground-state correlations, decaying as an stretched exponential, and the phase-independent $\eta = 2$ exponent which governs the mean value of the correlations [that decays as a power law, as in Eq. (83)]. Notice the remarkable difference between the arithmetic and typical averages of the correlations, a hallmark of the infinite-randomness character of the random singlet phases. Finally, the transition between these phases is

governed by the baryon-like SU(N) infinite-randomness fixed point.

B. Other infinite-randomness universality classes

Given the variety of tunneling exponent values ψ here found and its importance in characterizing the corresponding infinite-randomness fixed points, it is natural to inquire whether ψ can assume values different from the inverse of an integer $\frac{1}{N}$ with $N > 1$.

The simple answer is yes. Whenever the disorder in the coupling constants is long-range correlated [42] or deterministic [43], ψ can be even greater than $\frac{1}{2}$. In higher dimensions, ψ can be different as well due to a nontrivial coordination number [11,44]. However, these systems have additional ingredients not contained in our simpler model. Therefore, we ask whether "simple" random systems (i.e., systems in which the fixed-point coordination number is exactly 2 [45] with irrelevant short-range correlated disorder) can be governed by infinite-randomness fixed points with ψ^{-1} being different from an integer.

Novel values of ψ, different from the more conventional one of $\frac{1}{2}$ [3,5], were first found in certain random Heisenberg spin-S chains with $\psi = \frac{1}{m}$, with $m = 2S + 1$ being the number of different dimerized phases meeting at the multicritical point [6,7,16]. The corresponding universality class was named permutation symmetric due to the m distinct domains coexisting at the multicritical fixed point. However, the corresponding Hamiltonian required to ensure that all those phases meet at the same point is not known for $m > 4$ [46].

The first concrete model realizing the permutation-symmetric infinite-randomness universality class for $m > 4$ and meeting our criterion of being a "simple system" was the random antiferromagnetic SU(N)-symmetric spin chain [35]. It was shown to be governed by the baryonic infinite-randomness fixed points with $\psi = \psi_B = \frac{1}{N}$. Later, the SU(2)$_k$-symmetric anyonic chains [19] (with k being an odd integer) was the second realization of this universality class where $\psi = \frac{1}{k}$. Finally, the random SO(N)-symmetric spin chains here studied constitute yet another example. In all these systems, the SDRG decimation rules can be mapped into each other. The topological charge carried by the anyons plays the role of the domain-wall spins which, in turn, play the role of our totally antisymmetric spin representations in the SO(N) language. The corresponding sign of the couplings (ferro- or antiferromagnetic) between the anyons or between the domain-wall spins plays the role of the two angles found in our baryonic fixed points. In all cases, the tunneling exponent is determined by the probability p of having certain link configurations (ensuring a second-order decimation into a singlet). Thus, $p = \frac{N_2}{N_T}$, where N_2 is the total number of link configurations ensuring a singlet decimation and N_T is the total number of distinct configurations. From symmetry, these configurations are all equally probable and thus, N_T must be a multiple (which turns out to be $N - 1$) of N_2. Thus, $p = \frac{1}{N-1}$ is the inverse of an integer implying that the tunneling exponent $\psi = \frac{p}{1+p} = \frac{1}{N}$ is also the inverse of an integer. One might expect to find new values of ψ in SU(N)$_k$ anyonic

spin chains. However, this would only change $p = \frac{1}{N-1} \rightarrow \frac{1}{(k-1)(N-1)}$, which is also the inverse of an integer.

Another place to search for different values of ψ could be in random spin chains invariant under transformations of a discrete symmetry group. However, many quantum critical chains of random models like the Ising, and the various N-state Potts, clock, parafermionic, and Ashkin-Teller models were studied [5,47–50]. In all cases, the fraction of second-order decimations is $p = 1$, and thus $\psi = \frac{1}{2}$. Indeed, the ground state of the quantum critical Ising chain can be described as an RSP of an $SU(2)_2$ random anyonic chain [18]. It is plausible that the other models may also be described likewise.

Evidently, we cannot claim to have exhausted all possible infinite-randomness universality classes in simple one-dimensional systems. However, given the plethora of examples mentioned above, it is conceivable that the permutation-symmetric infinite-randomness universality class is the most general one capable of producing different values of ψ in one-dimensional systems fulfilling our criterion of "simple systems."

C. Entanglement entropy

The entanglement entropy of a finite chain segment of length L in the ground state of the mesonic RSPs here discussed can be calculated with the methods reviewed in Ref. [51]. It is given by

$$S_L = \left(\frac{1}{3} \log_2 D \right) \ln L, \tag{99}$$

where D is the dimension of the Hilbert space of an original spin. In our case $D = N$, which is the dimension of the fundamental $SO(N)$ or $Sp(N)$ representations. As for the baryonic phases, more than two spins are glued together to form a singlet and the determination of the entanglement entropy is more involved.

D. Weak disorder

The complete characterization of the weak-disorder case requires going beyond the method used in our work, which is tailor made to handle strong disorder. A nonconclusive hint about the weak-disorder limit can, however, be found within the SDRG approach. Typically, intermediate phases are found when the prefactor of the second-order decimation rules [see, for instance, Eqs. (56) and (57) for the $SO(N)$ case] are greater than one. Interestingly, it can be verified from these equations that for large N, the prefactor decays at the stable angular fixed points with $1/N$. With $N = 3, Q = 1$, one recovers the $S = 1$ case [14,15]. For this case, the prefactor is $4/3 > 1$ and there are indeed phases different from the RSPs discussed here. For $N > 3$ the prefactor is always less than one (recall that $Q \leqslant N/2$) at the angular fixed points, suggesting that weak disorder may be a relevant perturbation. Away from the angular fixed points, less can be said. As θ gets closer to the AKLT point (or any other point where the local 2-site gap closes), the prefactors on the decimation rules of K^{Υ}, which are θ dependent, increase. Again, the complete characterization requires other methods, such as perturbation theory in disorder, exact diagonalization, or density matrix renormalization group, and is left for future work.

E. Final remarks

The situations analyzed here have particular interest due to the possibilities of experimental realization [27] but do not necessarily exhaust all possibilities of symmetry enhancement in disordered spin chains. They do provide, however, a very large class of systems showing this phenomenon. The methodology developed here is also very embracing and provides the guidelines and tools for the study of more involved, exotic, or simply distinct scenarios. Exceptional Lie algebras remain to be studied, as well as Hamiltonians starting with larger dimensional representations of $SO(N)$ and $Sp(N)$ at each site. These problems are left for future research.

APPENDIX: DERIVATION OF THE Φ AND ξ LISTED IN TABLE III

In this Appendix, we derive the values of Φ and ξ listed in Table III. The derivation follows closely the $SU(N)$ SDRG steps studied in Ref. [35]. We use the notation $\mathcal{Q}$ and Q for the $SU(N)$ and $SO(N)$ Young tableaux, respectively, as well as J_i for the couplings of the $SU(N)$ chain. The $SU(N)$ decimation rules of Ref. [35], when the ground state is not a singlet, are

$$\tilde{J}_1 = \begin{cases} \xi J_1, & \mathcal{Q}_2 + \mathcal{Q}_3 < N, \\ \bar{\xi} J_1, & \mathcal{Q}_2 + \mathcal{Q}_3 > N, \end{cases} \tag{A1}$$

$$\tilde{J}_3 = \begin{cases} (1 - \xi) J_3, & \mathcal{Q}_2 + \mathcal{Q}_3 < N, \\ (1 - \bar{\xi}) J_3, & \mathcal{Q}_2 + \mathcal{Q}_3 > N, \end{cases} \tag{A2}$$

where $\xi = \frac{\mathcal{Q}_2}{\mathcal{Q}_2 + \mathcal{Q}_3}, \bar{\xi} = \frac{\bar{\mathcal{Q}}_2}{\bar{\mathcal{Q}}_2 + \mathcal{Q}_3}$, and $\bar{\mathcal{Q}} \equiv N - \mathcal{Q}$.

Building a correspondence between the $SO(N)$ and $SU(N)$ Young tableaux and comparing the decimation rules with Eq. (A1), each line of Table III is fixed. The first line, found in the positive $K^{(2)}$ region, is straightforward. If two $SO(N)$ representations Q_2 and Q_3 are added generating $\tilde{Q} = Q_2 + Q_3 \leqslant \mathrm{int}(\frac{N}{2})$, the correspondence with $SU(N)$ representations is immediate, that is, $Q_{2,3} = \mathcal{Q}_{2,3}$ and $\tilde{Q} = \tilde{\mathcal{Q}}$, and the decimation rules are exactly the same as in Eq. (A1).

If, on the other hand, $Q_2 + Q_3 > \mathrm{int}(\frac{N}{2})$ (second line of Table III), it follows that $\tilde{\mathcal{Q}} = \mathcal{Q}_2 + \mathcal{Q}_3 < N$ in the $SU(N)$ language. When translated to the $SO(N)$ tableaux, $\tilde{Q} = N - Q_2 - Q_3$. It follows, therefore, that $N - Q_2 - Q_3 = \mathcal{Q}_2 + \mathcal{Q}_3$. This transformation of representations is achieved by choosing $\xi_1 = \xi_3 = -1$, fixing the next entry of Table III.

Finally, for the decimations of negative $K^{(2)}$ (last line of Table III), the SU(N)-SO(N) identifications $\mathcal{Q}_2 = N - Q_2$ and $\mathcal{Q}_3 = Q_3$ are made. Notice also that we chose $Q_2 < Q_3$. This correspondence can be seen by comparing the Hamiltonian at the SU(N)-invariant point $\theta = -\frac{\pi}{4}$. By performing the RG decimation using the SU(N) language, the ground state is $\tilde{\mathcal{Q}} = N - Q_2 + Q_3$. From the choice $Q_3 > Q_2$, $\tilde{\mathcal{Q}} > N$, and within SU(N), we get $\tilde{\mathcal{Q}} = Q_3 - Q_2$. Putting everything together,

Eq. (A1) returns

$$\tilde{J}_1 = \frac{\bar{\mathcal{Q}}_2}{\bar{\mathcal{Q}}_2 + \bar{\mathcal{Q}}_3} J_1 = \frac{N - \mathcal{Q}_2}{2N - \mathcal{Q}_2 + \mathcal{Q}_3} J_1$$

$$= \frac{Q_2}{N - Q_2 + Q_3} J_1. \tag{A3}$$

This gives the value of Φ_1 listed in the third line of Table III. The derivation of Φ_3 follows similar steps.

[1] S. Sachdev, *Quantum Phase Transitions* (Cambridge University Press, 2001).

[2] F. Iglói and C. Monthus, Phys. Rep. **412**, 277 (2005).

[3] D. S. Fisher, Phys. Rev. B **50**, 3799 (1994).

[4] P. Mohan, R. Narayanan, and T. Vojta, Phys. Rev. B **81**, 144407 (2010).

[5] D. S. Fisher, Phys. Rev. B **51**, 6411 (1995).

[6] K. Damle, Phys. Rev. B **66**, 104425 (2002).

[7] K. Damle and D. A. Huse, Phys. Rev. Lett. **89**, 277203 (2002).

[8] J. A. Hoyos, C. Kotabage, and T. Vojta, Phys. Rev. Lett. **99**, 230601 (2007).

[9] J. Hooyberghs, F. Iglói, and C. Vanderzande, Phys. Rev. Lett. **90**, 100601 (2003); F. Iglói and C. Monthus, Eur. Phys. J. B **91**, 290 (2018); T. Vojta and J. A. Hoyos, Europhys. Lett. **112**, 30002 (2015).

[10] T. Vojta and J. A. Hoyos, Phys. Rev. Lett. **112**, 075702 (2014).

[11] O. Motrunich, S.-C. Mau, D. A. Huse, and D. S. Fisher, Phys. Rev. B **61**, 1160 (2000).

[12] I. A. Kovács and F. Iglói, Phys. Rev. B **83**, 174207 (2011).

[13] R. A. Hyman and K. Yang, Phys. Rev. Lett. **78**, 1783 (1997).

[14] C. Monthus, O. Golinelli, and T. Jolicoeur, Phys. Rev. Lett. **79**, 3254 (1997).

[15] C. Monthus, O. Golinelli, and Th. Jolicoeur, Phys. Rev. B **58**, 805 (1998).

[16] G. Refael, S. Kehrein, and D. S. Fisher, Phys. Rev. B **66**, 060402(R) (2002).

[17] V. L. Quito, J. A. Hoyos, and E. Miranda, Phys. Rev. B **94**, 064405 (2016).

[18] N. E. Bonesteel and K. Yang, Phys. Rev. Lett. **99**, 140405 (2007).

[19] L. Fidkowski, H.-H. Lin, P. Titum, and G. Refael, Phys. Rev. B **79**, 155120 (2009).

[20] V. L. Quito, J. A. Hoyos, and E. Miranda, Phys. Rev. Lett. **115**, 167201 (2015).

[21] C. Dasgupta and S.-k. Ma, Phys. Rev. B **22**, 1305 (1980).

[22] S.-k. Ma, C. Dasgupta, and C.-k. Hu, Phys. Rev. Lett. **43**, 1434 (1979).

[23] R. N. Bhatt and P. A. Lee, Phys. Rev. Lett. **48**, 344 (1982).

[24] T. Vojta, J. Phys. A: Math. Gen. **39**, R143 (2006).

[25] In general, symmetry emergence denotes a crossover in which the low-energy long-wavelength physics of a Hamiltonian is governed by a larger symmetry group than that governing the short-wavelength regime [7,19,52–62].

[26] K. I. Kugel and D. I. Khomskii, Sov. Phys. Usp. **25**, 231 (1982).

[27] V. L. Quito, P. L. S. Lopes, J. A. Hoyos, and E. Miranda, arXiv:1711.04781.

[28] A. V. Gorshkov, M. Hermele, V. Gurarie, C. Xu, P. S. Julienne, J. Ye, P. Zoller, E. Demler, M. D. Lukin, and A. M. Rey, Nat. Phys. **6**, 289 (2010).

[29] F. Iachello, *Lie Algebras and Applications* (Springer, Berlin, 2006).

[30] We can assume $a < b$ if we define $L^{ab} = -L^{ba}$ whenever $a > b$.

[31] H.-H. Tu, G.-M. Zhang, and T. Xiang, Phys. Rev. B **78**, 094404 (2008).

[32] K. Yang and R. N. Bhatt, Phys. Rev. Lett. **80**, 4562 (1998).

[33] A. R. Edmonds, *Angular Momentum in Quantum Mechanics* (Princeton University Press, 1996).

[34] R. Feger and T. W. Kephart, arXiv:1206.6379.

[35] J. A. Hoyos and E. Miranda, Phys. Rev. B **70**, 180401(R) (2004).

[36] One way of computing the coefficient of the quadratic term is by adding Eqs. (15) and (16), which makes the resulting object SU(N) invariant. By summing Eqs. (7) and (8) of Ref. [31], one obtains the coefficient of the quadratic term.

[37] Sometimes, a multiplicity label β is included to account for possible degeneracies coming from the Clebsch-Gordan series. Such distinction is not important for our purposes here.

[38] E. Westerberg, A. Furusaki, M. Sigrist, and P. A. Lee, Phys. Rev. B **55**, 12578 (1997).

[39] I. Affleck, T. Kennedy, E. H. Lieb, and H. Tasaki, Phys. Rev. Lett. **59**, 799 (1987).

[40] We use the term antiferromagnetic here in the loose sense that there is a tendency to form singlets. Actually, there is never true antiferromagnetic order.

[41] J. C. Xavier, J. A. Hoyos, and E. Miranda, Phys. Rev. B **98**, 195115 (2018).

[42] H. Rieger and F. Iglói, Phys. Rev. Lett. **83**, 3741 (1999).

[43] A. P. Vieira, Phys. Rev. Lett. **94**, 077201 (2005).

[44] T. Senthil and S. Sachdev, Phys. Rev. Lett. **77**, 5292 (1996).

[45] For instance, random spin ladders have bare coordination numbers different from 2. However, it was shown that the fixed-point Hamiltonian is one-dimensional; i.e., the low-energy physics is that of a spin chain [63].

[46] The possibility of fine-tuning raised by the authors was the addition of next-nearest-neighbor interactions. However, this seems unlikely in view of the results of Ref. [63].

[47] T. Senthil and S. N. Majumdar, Phys. Rev. Lett. **76**, 3001 (1996).

[48] R. Santachiara, J. Stat. Mech.: Theory Exp. (2006) L06002.

[49] F. Hrahsheh, J. A. Hoyos, and T. Vojta, Phys. Rev. B **86**, 214204 (2012).

[50] H. Barghathi, F. Hrahsheh, J. A. Hoyos, R. Narayanan, and T. Vojta, Phys. Scr. **T165**, 014040 (2015).

[51] G. Refael and J. E. Moore, J. Phys. A: Math. Theor. **42**, 504010 (2009).

[52] A. B. Zamolodchikov, Int. J. Mod. Phys. A **04**, 4235 (1989).

[53] A. Rahmani, X. Zhu, M. Franz, and I. Affleck, Phys. Rev. Lett. **115**, 166401 (2015).

[54] J. Schmalian and C. D. Batista, Phys. Rev. B **77**, 094406 (2008).

[55] R. Coldea, D. A. Tennant, E. M. Wheeler, E. Wawrzynska, D. Prabhakaran, M. Telling, K. Habicht, P. Smeibidl, and K. Kiefer, Science **327**, 177 (2010).

[56] T. Senthil, A. Vishwanath, L. Balents, S. Sachdev, and M. P. A. Fisher, Science **303**, 1490 (2004).

[57] T. Grover, D. N. Sheng, and A. Vishwanath, Science **344**, 280 (2014).

[58] C. D. Batista and G. Ortiz, Adv. Phys. **53**, 1 (2004).

[59] P. Chen, Z.-L. Xue, I. P. McCulloch, M.-C. Chung, C.-C. Huang, and S.-K. Yip, Phys. Rev. Lett. **114**, 145301 (2015).

[60] E. Zohar, J. I. Cirac, and B. Reznik, Rep. Prog. Phys. **79**, 014401 (2016).

[61] C. Itoi and M.-H. Kato, Phys. Rev. B **55**, 8295 (1997).

[62] H.-H. Lin, L. Balents, and M. P. A. Fisher, Phys. Rev. B **58**, 1794 (1998).

[63] J. A. Hoyos and E. Miranda, Phys. Rev. B **69**, 214411 (2004).